



A multi-environmental tracer study to determine groundwater residence times and recharge in a structurally complex multi-aquifer system

5 Cornelia Wilske^{1,2}, Axel Suckow², Ulf Mallast¹, Christiane Meier³, Silke Merchel⁴, Broder Merkel⁵,
Stefan Pavetich^{5,6}, Tino Rödiger⁷, Georg Rugel⁵, Agnes Sachse⁷, Stephan M. Weise¹, Christian Siebert¹

¹ Helmholtz Centre for Environmental Research, Dept. Catchment Hydrology, Halle/Saale, 06120, Germany.

² CSIRO Land and Water, Urrbrae (SA), 5064, Australia

³ UBA Umweltbundesamt, Dessau-Roßlau, 06844, Germany

⁴ Helmholtz-Zentrum Dresden-Rossendorf, Dresden, 01328, Germany

10 ⁵ TU Bergakademie Freiberg/Sachs., 09599, Germany

⁶ Australian National University, Dept. Nuclear Physics, Canberra (ACT), 2609, Australia

⁷ Helmholtz Centre for Environmental Research, Dept. Computational Hydrology, Leipzig, 04318, Germany

Correspondence to: Christian Siebert (Christian.siebert@ufz.de)

Abstract. Despite being the main drinking water resource for over five million people, the water balance of the Eastern
15 Mountain Aquifer system on the western side of the Dead Sea is poorly understood. The regional aquifer consists of
fractured and karstified limestone — aquifers of Cretaceous age and can be separated in Cenomanian aquifer (upper aquifer)
and Albian aquifer (lower aquifer). Both aquifers are exposed along the mountain ridge around Jerusalem, which is the main
recharge area. From here, the recharged groundwater flows in a highly karstified aquifer system towards the east, to
discharge in springs in the Lower Jordan Valley and Dead Sea region. We investigated the Eastern Mountain Aquifer system
20 on groundwater flow, groundwater age and potential mixtures, and groundwater recharge. We combined ³⁶Cl/Cl, tritium and
the anthropogenic gases SF₆, CFC-12 and CFC-11, CFC-113 as “dating” tracers to estimate the young water components
inside the Eastern Mountain Aquifer system. By application of lumped parameter models, we verified young groundwater
components from the last 10 to 30 years and an admixture of a groundwater component older than about 70 years.
Concentrations of nitrate, Simazine® (Pesticide), Acesulfame K® (artificial sweetener) and Naproxen® (drug) in the
25 groundwater were further indications of infiltration during the last 30 years. The combination of multiple environmental
tracers and lumped parameter modelling helped to understand the groundwater age distribution and to estimate recharge
despite scarce data in this very complex hydrogeological setting. Our groundwater recharge rates support groundwater
management of this politically difficult area and can be used to inform and calibrate ongoing groundwater flow models.



30 1 Introduction

About 20 percent of the Earth's land surface is covered by carbonate-karst or sulphate aquifers and serve as the primary water resource for at least 25% of the world's population. In addition, about 20% of the world's karst systems are in (semi-) arid areas, whose water scarcity is aggravated by strong population growth (Ford and Williams, 2007). Karst systems represent abundant, but highly variable water resources whose extremely heterogeneous and anisotropic flow behaviour prevents exact predictions regarding mass transport and the usable water quantities (Bakalowicz, 2005). Nevertheless, the water balance stays the basic requirement for sustainable management and protection of any water resources.

Environmental tracers play an important role in sustainable water management strategies because they allow to estimate the groundwater age distribution with depth and together with simple lumped parameter models to quantify groundwater infiltration rates (IAEA, 2006; Solomon et al., 1995; Vogel, 1967). Especially in karst aquifers, wide ranges of residence times are observable due to the strongly heterogeneous hydraulic system, allowing water to rapidly flow through conduits and fractures and very slowly flow through the small pores of the matrix. That leads to large heterogeneities in the groundwater age distribution requiring hence especially in karst the application of multiple tracers to constrain the age distribution. We define young groundwater as having measurable concentrations of anthropogenic tracers and therefore a mixing component recharged after about 1950, while in old groundwater these tracers are not detectable (e.g. Plummer et al. 1993, Cook & Herczeg 2000, Hinsby et al. 2001a). The atmospheric tracer CFC-11, CFC-12, CFC- 113, SF₆ (sulphur hexafluoride) and ³⁶Cl/Cl and Tritium from bomb-tests or anthropogenic organic trace pollutants like pesticides, sweeteners or drugs are increasingly used as tracers of young groundwater (IAEA 2006). Gas tracers like CFCs and SF₆ move through the unsaturated zone primary by diffusion, leading to a time lag at the water table compared to the atmosphere (Cook and Solomon, 1995; Cook et al., 1995). A time lag is also possible for the water bound tracers tritium and ³⁶Cl, since the advection through the unsaturated zone may take decades (Lin and Wei, 2006; Suckow et al., 1993) and in infiltration areas dominated by sand or clay, water bound tracers are generally slower than gas tracers (Cook et al., 1995; Solomon et al., 1992). This can be very different in karst systems, where preferential flow in karst “tubes” allows fast recharge to the water table and fluctuations of groundwater level may allow further gas exchange thereafter.

The deconvolution of measured tracer concentrations into recharge rates therefore needs modelling. If age of water would be known as function of depth, any flow model could be directly constrained and the recharge rates deduced. However, the “idealized groundwater age”, which is often understood as the time span an imaginary water parcel needs between infiltrating at the groundwater surface and being sampled at a well or spring (Suckow, 2014a) is not directly measurable. Also groundwater mixes both on its natural flow and during sampling in the well. Therefore, simple lumped parameter models (LPM) are used to interpret the measured tracer concentrations as mean residence times (MRT) via a convolution integral, which in combination with the underlying assumptions on the flow system allow deducing recharge rates. We



applied the piston flow model (PM), the dispersion model (DM) and the partial exponential model (PEM) to approximate the age distribution in our groundwater samples.

In our study, over five million people are reliant on drinking water from the Eastern Mountain Aquifer system (EMA) in the western Dead Sea catchment. Unequal distribution of both borehole information lead to poor and limited data for studying the aquifer system. Previous studies considered age dating tracers to quantify water movement and flow velocity within the
65 the aquifer system. Previous studies considered age dating tracers to quantify water movement and flow velocity within the EMA and associated aquifers. Paul et al. (1986) and Yechieli et al. (1996) studied $^{36}\text{Cl}/\text{Cl}$ to detect very old groundwater brines in the Dead Sea area. In contrast young-age dating tracers such as Tritium or anthropogenic trace gases (CFCs and SF₆) were used to quantify the duration of water flow from the recharge area to the springs (Yechieli et al. 1994; Lange 2011). Environmental tracer investigations of the main Cretaceous aquifers (Upper Cenomanian and Albian) in the western
70 Dead Sea catchment attempted to quantify the duration of water flow from the recharge area to the springs in the mountain region in the foreland of the Dead Sea coast. The young-age dating tracers demonstrated a large young groundwater fraction with a mean residence time of less than 30 years in the springs of the mountain region and fast connections to the recharge area. All previous studies together show large heterogeneities in the groundwater age distribution (Avrahamov et al., 2018).

In this study we combine for the first time in this area bomb-derived ^{36}Cl , anthropogenic organic trace substances and
75 environmental tracers like tritium, CFCs, SF₆ in combination with lumped parameter models to interpret the distribution of these tracers to quantify recharge. Maloszewski & Zuber (1982, 1993, 1996) have shown that LPM are a useful tool for interpreting tracer data obtained at separate sampling sites when it is not possible to use distributed parameter models, as the latter require more detailed and often unavailable knowledge of distributed parameters for the investigated system. In detail this work aims to (i) validate young rainwater input and fast groundwater movement via karst conduits, related to rapid flow
80 paths from the recharge area; (ii) to quantify the time lag of gas tracers in the unsaturated zone; (iii) to quantify groundwater mixing of groundwater components with different age via lumped parameter models and (vi) to estimate groundwater recharge and support calculations of future groundwater resource development.

1.1 Study Area

The study area, which represents the western surface drainage basin of the Dead Sea, is embedded in a region that is
85 morphologically and geologically dominated by the tectonic processes associated with the Jordan-Dead Sea Rift, being active since the late Oligocene (Garfunkel et al., 1981; Rosenfeld and Hirsch, 2005). The western rift fault separates the Cretaceous aquifer formations that form the Graben shoulder from the deeply subsided Graben and its Quaternary filling. In addition, rift tectonics induced a series of faults within the western Graben Shoulder, resulting in down-faulted blocks, which find their surface expression in a strong morphological gradient. Within less than 25 km, the land surface drops from +800 m
90 msl. in the west to sea level at the rift margin and with a terminal step to -430 m msl. at the Dead Sea in the east (Fig. 1).



The semi-arid to arid Mediterranean climate leads to precipitation during the winter season, but with a strong decline from west to east due to which the study area can be divided into three hydrological zones: (i) the recharge area in the upland that receives annually up to 580 mm of precipitation; (ii) the transition zone occupying the hillsides of the upland down to the rift margin, receiving 100-400 mm/a and (iii) the major discharge area of the groundwater in the Lower Jordan Valley/Dead Sea area, receiving less than 100 mm/a of precipitation.

The Graben shoulder hosts a thick aquifer system that is mainly built of fractured and in layers karstified Upper Cretaceous lime- and dolostones, which are overlain by a Senonian chalky aquitard (Weinberger and Rosenthal 1996; Kronfeld and Rosenthal 1987). A marly aquiclude (Lower Cenomanian) divides the system into a Lower Aquifer (Albian) and Upper Aquifer (Upper Cenomanian). Occurring impervious beds in the Upper Aquifer permit the development of a perched and locally important aquifer (Turonian), being built of homogenous and fissured limestones and holds springs, which emerge in deeply incised valleys within the transition zone, (e.g. Wadi Qilt; Fig. 2). While all aquifer units are recharged in the mountain area, the natural discharge of the two regional aquifers occurs through springs at the base of the Graben Shoulders, where the groundwaters leave the aquifers and approach the prevalently impervious Quaternary Graben filling.

Subsequently, groundwater emerges along the shore in spring clusters, forming ecologically important oasis such as Ein Feshkha. Where groundwaters can percolate into the Quaternary sediments, they intensely dissolve the contained evaporite minerals (anhydrite, halite, aragonite) and get saline on their way to the lake shore. In addition, the chemical and isotopic composition of approaching fresh groundwaters get systematically modified by admix of brines, already in the vicinity of the major rift fault (Ghanem, 1999; Katz and Kolodny, 1989; Khayat et al., 2006a; Khayat et al., 2006b; Klein-BenDavid et al., 2004; Möller et al., 2007; Siebert et al., 2014; Starinsky and Katz, 2014; Stein et al., 1997; Yechieli, 2000). Groundwater recharge rates are controlled by climate conditions and have been investigated earlier to force regional groundwater models (Gräbe et al., 2013; Guttman et al., 2004; Schmidt et al., 2014; Yellin-Dror et al., 2008), which allowed a detailed insight of the regional groundwater flow dynamics.

Human groundwater abstraction takes place mainly in the mountain ridge inside the recharge area and along the transition to the Jordan Valley. This unequal distribution of the sampling possibilities led to a data scarcity for the entire central area of the aquifer, which is also visible in Figure 1.

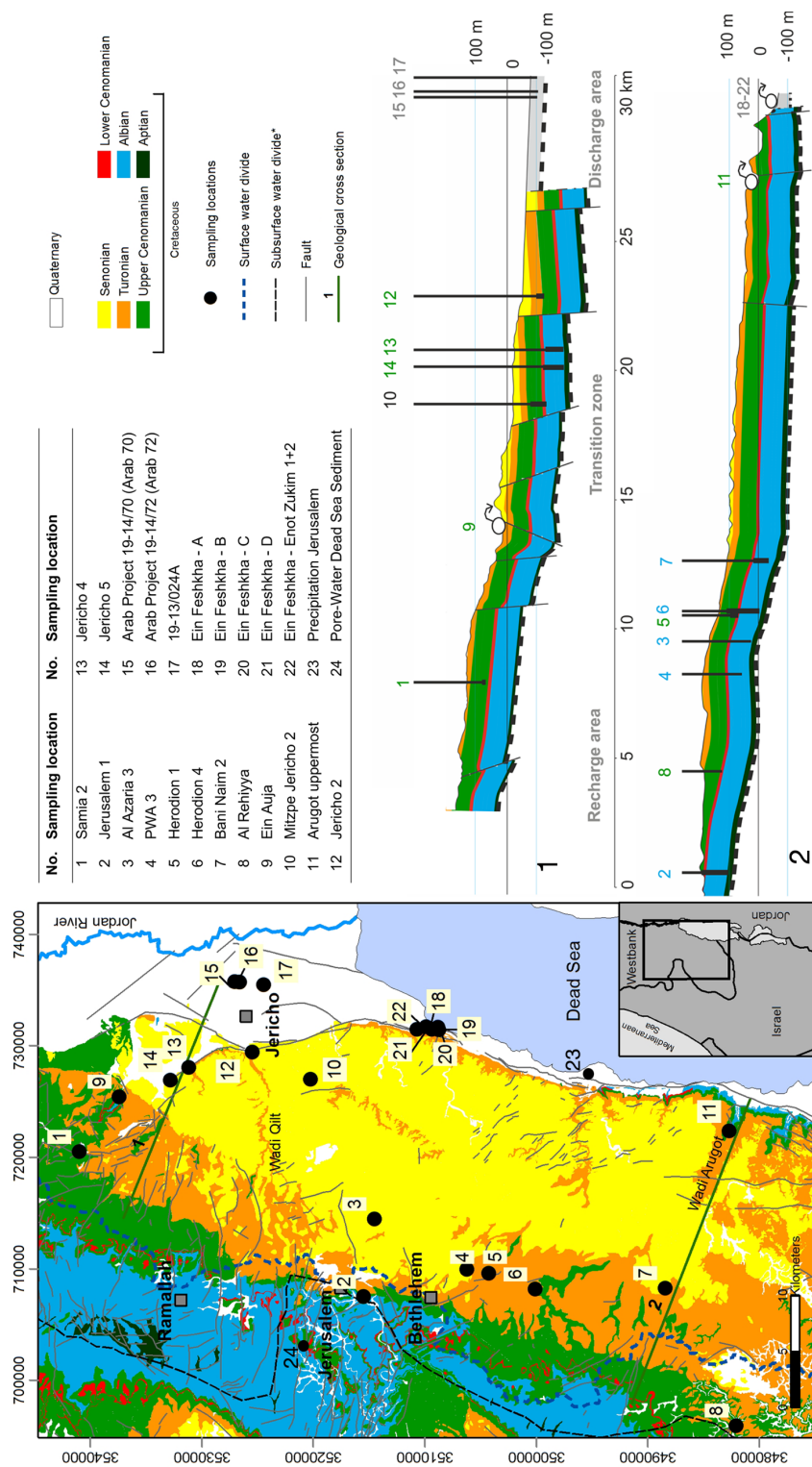


Figure 1: shows the location of the study site including geological information based on (Begin, 1974; Mor and Burg, 2000; Raz, 1986; Roth, 1973; Shachnai, 2000; Sneh and Avni, 2011; Sneh and Roth, 2012). Coordinates: UTM WGS84 Z36N.



2 Materials and Methods

2.1 Fundamentals of the Method

120 Age distributions of young groundwater can be characterized by applying anthropogenic trace gases like CFC-11, CFC-12, CFC-113 and SF₆ in lumped parameter models if an input function is available. For the last 6 decades, that function can be derived for gas tracers from (i) their known concentrations in the atmosphere (Fig.2), (ii) the observation that they are well mixed in the atmosphere, and (iii) that their solubility at the temperature of recharge is known from Henry's Law (Plummer & Busenberg 1999). The large-scale production of CFC-12 and CFC-11 (both used as cooling fluid) started in the early 125 1940s while production of CFC-113 started in 1960s only. Inevitably they leaked into the environment, with atmospheric concentrations rising until the 1990s, when their moratorium took effect. Another industrial gas SF₆, widely used as electrical insulator is detectable in the atmosphere since 1960s with still exponentially rising concentrations. Atmospheric concentrations of SF₆ and the CFCs for the period 1953-2006 (Fig. 2) are derived from Plummer et al. (2006). Since gas solubility in recharging precipitation depends on temperature and atmospheric pressure, the average air temperature of the 130 winter season in the study area (15°C) was used for the former and an altitude of 700 m asl., which is the average altitude of the infiltration area, was used for the latter. The rain water salinity was set to 0 [%] since rain water is low mineralised.

Tritium (³H) is the naturally-occurring isotope of hydrogen and is mainly produced by fast secondary neutrons from cosmic radiation. It decays to ³He with a half-life time of 12.32 ± 0.02 a (Lucas and Unterweger, 2000), making ³H usable for groundwater age dating in a time frame of <40 years (e.g. (Cook and Solomon, 1997; Schlosser et al., 1988; Solomon et al., 135 1992; Sültenfuß and Massmann, 2004), including quantifying changes of measured ³He/⁴He ratios in groundwater. At the study area, observation of tritium in precipitation (GNIP stations Beer Sheva, Bet Dagan and Tirat Yael (IAEA/WMO, 2017)) were available for 1960-2001 only, while input data are required until 2014. We therefore applied tritium data of Vienna station, Austria (IAEA/WMO, 2017), which are adjusted to the longitudinal and latitudinal difference by a factor of 0.4 to match the Israel stations (Fig. 2). For the synoptic tracer plots the decay correction is to October 31, 2013. The pre- 140 bomb input value for tritium was set to a mean tritium concentration of 3 TU obtained from the GNIP data base (IAEA/WMO, 2017).

³⁶Cl is produced naturally via cosmic-ray and solar protons induced nuclear reactions of argon in the atmosphere and of ³⁵Cl in marine aerosols (Alvarado et al., 2005). However, comparable to ³H, the atmospheric concentration of "bomb" ³⁶Cl peaked during the 1950s as an effect of nuclear weapon tests and was washed out from the atmosphere until the end of the 145 1960s. The ³⁶Cl bomb peak precedes the tritium peak by half a decade. The ³⁶Cl input curve for our study area (Fig. 2) was obtained from Iceland ice core measurements from Synal et al. (1990), which were corrected to the location of the study area applying a latitudinal correction with a factor of three, according to (Heikkilä et al. (2009), who modelled ³⁶Cl fall-out for



different latitudes. Natural “pre-bomb” concentration of $^{36}\text{Cl}/\text{Cl}$ was assumed to be 10^{-14} , which is based on $^{36}\text{Cl}/\text{Cl}$ in rainwater, sampled during winter 2014/2015 with an average value of $^{36}\text{Cl}/\text{Cl}=8\times 10^{-15}$.

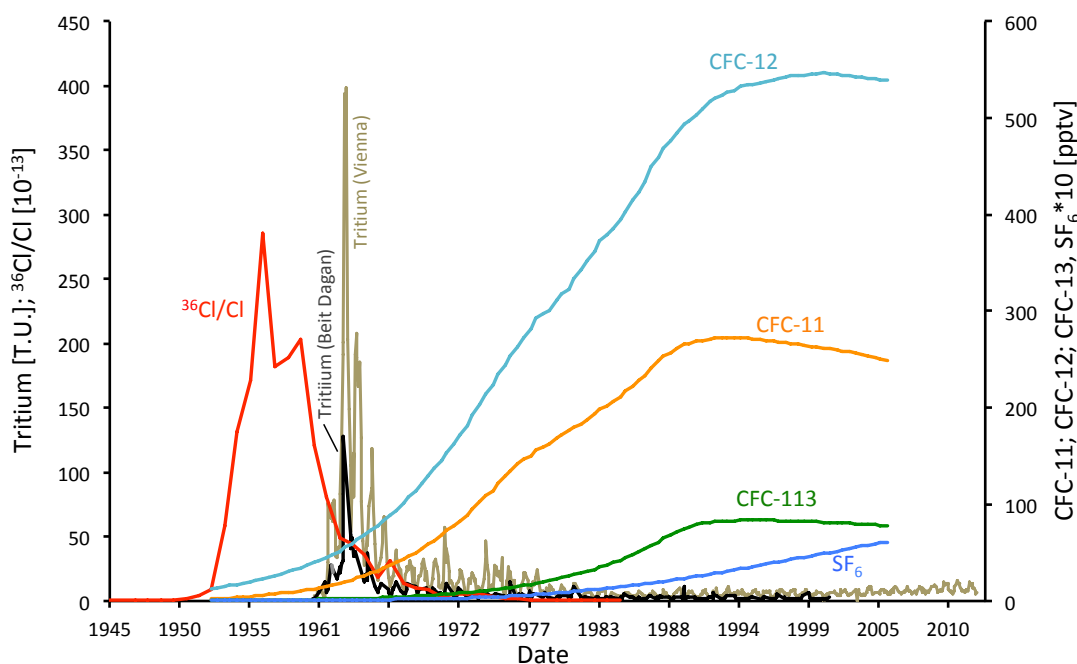


Figure 2: Atmospheric input curves of $^{36}\text{Cl}/\text{Cl}$ (^{36}Cl obtained from Dye-3 ice core, Synal et al. (1990)), SF_6 and CFCs (Plummer et al., 2006) and decay-corrected Tritium in rain water of Beit Dagan and Vienna (IAEA/WMO, 2017).

150 Most studies to estimate groundwater age with ^{36}Cl base on the half-life of ^{36}Cl (0.301 ± 0.015 Ma) (Nica et al., 2006) and consider time frames $>100,000$ years (Bentley et al., 1986; Davis et al., 1983; Love et al., 2000; Mahara et al., 2012; Müller et al., 2016). Studies using ^{36}Cl from the atmospheric bomb peak to estimate groundwater age of the last decades are much less-frequent (Alvarado et al., 2005; Lavastre et al., 2010; Rebeix et al., 2014; Tosaki et al., 2010; Tosaki et al., 2007)).

Anthropogenic organic trace pollutants in groundwater are associated to nutrition, medication or agricultural and industrial development. During the last decades, artificial sweeteners played an important role as a surrogate in the nutrition industry. Particularly Acesulfame K® (ACE-K) is used since the 1990s and is stable against waste water treatment (WWT) processes, making it an ideal tracer for domestic wastewater. A second chemical marker for human intake is Naproxen® (NAP), widely applied as anti-inflammatory drug since the 1980s. Though NAP is partly eliminated during WWT and may be adsorbed along flow-paths to sediments (Chefet et al., 2008; Yu, et al., 2008; Teijón et al., 2013), it occurs in effluents of sewage plants and increasingly in natural waters (Arany et al., 2013). Contrasting that, ACE-K is hydrophilic (e.g. Buerge & Poiger, 2011) and inert against degradation, which makes it a valuable substance to trace transport from the recharge- towards the

160



discharge area. In addition to the urban indicators, pesticide traces in groundwater were used to identify the agricultural contributions to the water resources. Simazine®, which is available since the 1950s is one of the most applied herbicides and absorbs to soil where it may be eliminated through bacterial degradation. However, the use of Simazine® is phased out in
165 Israel since 2012-2014 (Berman et al., 2014). Nitrate is another indicator for anthropogenic input, whose distribution in groundwater originates from nitrification of NH_4 during WWT and as a fertilizer excess in agriculture.

2.1 Sampling and analytical methods

In the study area, 22 groundwater samples were taken from springs and active wells (sampling locations in Fig. 1, Tab. 1) after reaching stable conditions for temperature, electrical conductivity and pH. Major anion samples were filled into HD-PE
170 bottles after passing a $0.45\ \mu\text{m}$ cellulose acetate filter. Samples for cations were acidified using HNO_3 . Samples for ^{36}Cl analyses are filled into 500 ml HD-PE bottles, which have been specifically pre-cleaned using ultrapure HNO_3 . Samples for ^{36}Cl analyses were acidified with HNO_3 . Following the methodology described in Oster et al. (1996), sampling for CFCs and SF_6 was performed using glass bottles fully submerged in tins, filled with sampling water. Tritium samples were collected in
175 500 ml HD-PE bottles. Organic trace elements were sampled in pre-cleaned, methanol flushed 1000 ml brown glass bottles with the use of a glass microfiber filter ($0.7\ \mu\text{m}$).

Major element analyses in water samples were performed at the Helmholtz-Centre for Environmental Research (UFZ) by using matrix adjusted ICP-AES (Spectro Arcos) for Ca^{2+} , Mg^{2+} , Na^+ , K^+ and Sr^{2+} and by using ion chromatography (Dionex ICS-2000) for Cl^- , Br^- and SO_4^{2-} . Bicarbonate was determined *in situ* by titration. Analyses of ^{36}Cl were carried out in
180 Helmholtz-Zentrum Dresden-Rossendorf at the accelerator mass spectrometry (AMS) facility DRESDEN AMS (DREAMS) (Akhmadaliev et al., 2013). The main preparation steps (Conard et al., 1986) consist of: (i) precipitation of chloride via adding AgNO_3 solution (10%) and subsequent dissolution of the AgCl in $\text{NH}_{4\text{aq}}$; (ii) separation of chlorides from sulphates by co-precipitation of BaSO_4 with BaCO_3 (CO_2 from air) using saturated BaNO_3 solution and filtration through a syringe filter made of polyvinylidene fluoride (pore size: $0.45\ \mu\text{m}$); (iii) re-precipitation of AgCl in the filtrate with nitric acid. ^{36}Cl is measured with AMS relative to the stable Cl isotopes, ^{35}Cl and ^{37}Cl (Pavetich et al., 2014; Rugel et al., 2016), and is given as
185 ratio $^{36}\text{Cl}/(^{37}\text{Cl}+^{35}\text{Cl})$ (termed $^{36}\text{Cl}/\text{Cl}$ in the text). All data is normalized to the standards SM-Cl-12 and SM-Cl-13 (Merchel et al., 2011).

Tritium sample preparation and measurement were conducted by the isotope hydrology group at UFZ, following the preparation steps of Trettin et al. (2002) by first enriching a 400 ml water sample electrolytically and measure it via liquid scintillation counting with a detection limit of 0.5 TU.
190 CFCs and SF_6 were analysed in the Spurenstofflabor Dr. Harald Oster (Wachenheim, Germany) by Gas Chromatography (Bullister and Weiss, 1988; Oster et al., 1996). Measurements of organic trace elements were conducted with High Pressure Liquid Chromatography-Mass Spectrometry (HPLC-MS) at the UFZ. To transport the samples to the lab, organic components were stabilized by solid phase extraction (SPE) on cartridges containing a polar-modified polystyrene-divinylbenzene copolymer (Chromabond Easy, Machery-Nagel). At the lab, analytes were eluted with methanol and



195 measured with HPLC-MS/MS (Agilent 1000, Agilent Technologies, Germany; coupled with an API2000 mass spectrometer
(AB Sciex, Germany)). Limits of detections are 1 µg/l, 0.6 µg/l and 0.3 µg/l for Naproxen®, Acesulfame K® and
Simazine®, respectively. Analytical Results are given in Table 1.

2.1 Lumped parameter model “LUMPY”

LPM are pre-defined analytical solutions of simplified flow systems. They describe the tracer output mathematically with a
200 convolution integral that combines the tracer input history, weighed with the age distribution valid for the flow system in
question (Maloszewski and Zuber, 2002; Małoszewski and Zuber, 1982).

Mathematically all lumped parameter models for steady-state flow systems with a time-variable tracer input are convolution
integrals (Equation 1):

$$C_{out}(t) = \int_0^{\infty} C_{in}(t - t') \exp(-\lambda t') g(t') dt' \quad (1)$$

205 where t = calendar time; t' = transit time of the tracer; C_{out} = output concentration; C_{in} = input concentration; and $g(t')$ =
weighting function or system response function. All weighting functions of all models are normalized, following Equation
(2):

$$\int_0^{\infty} g(t') dt' = 1 \quad (2)$$

The mean residence time (MRT) is the main fitting parameter, while some models (e.g. dispersion model) require additional
210 parameters like (i) Péclet number, (ii) top and bottom of screened section or (iii) saturated thickness of the aquifer. Input data
are (i) regional atmospheric tracer input curves and (ii) selected hydrogeological characteristics such as the infiltration
temperature and elevation.

In this study the LPM code LUMPY (Suckow, 2012) was used to implement the convolution integral for flow systems that
can be described by the piston flow model (PM), the exponential model (including the partial exponential model PEM) and
215 the dispersion model (DM).

The PM describes the movement of a water parcel along a defined flow path from the aquifer surface towards the spring or
well filter, neglecting any mixing, dispersion or diffusion. The DM characterizes transport influenced by dispersion and
advective flow. The relative magnitude of both is expressed as the Péclet number Pe (Equation 3):

$$Pe = l \cdot v / D \quad (3)$$

220 where l is the flow length of the system under consideration, v is the velocity and D is the dispersion constant (Huysmans
and Dassargues, 2005). In our model approach, best fits were obtained by applying a Péclet number of 30, characterizing
dominantly advective transport.

The PEM is related to the exponential model (EM). Based on homogenous infiltration into a homogeneous aquifer as in
(Vogel, 1967), the PEM describes mixing of those flow lines reaching the filter screen of a well. In the special case where
225 the filter screen extends over the whole thickness of the aquifer the PEM is equivalent to the exponential model (EM), and



the MRT is the only fitting parameter. The mathematical equation of DM, EM and PEM are described in Maloszewski and Zuber (1982), Maloszewski and Zuber (2002) and (Jurgens et al., 2016).

Table 1. sampling locations and analytical results.

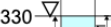
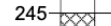
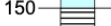
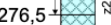
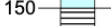
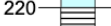
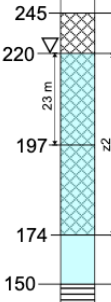
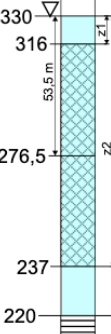
No	Station	ID	Sampling date	x.utm	y.utm	Elevation [m NN]	USZ [m]	pH	EH [mV]	T [°C]	EC [µS/cm]	NO ₃ [mg/l]	Cl [mg/l]	³⁵ Cl/Cl [10 ⁻³]	CFC-11 [fmol/l]	CFC-12 [fmol/l]	CFC-113 [fmol/l]	SF ₆ [fmol/l]	Trilium [T.U.]	Simazine [ng/l]	Acesulfame K [ng/l]	Naproxene [ng/l]		
Wells - recharge zone (Cenomanian)																								
1	Samia 2	12513	10.11.2012	720508	3541480	420.3	175	7.5	429	22.3	476	16.5	38.0	1.57 ± 0.08	2.3 ± 0.3	1.2 ± 0.1	0.19 ± 0.05	1.0 ± 0.2	2.1 ± 0.5	3.8	0.4	13.7	137.4	
	Samia 2	13056	22.05.2013					7.5	349	23.6	479	16.3	34.8							4.9				
5	Hendon 1	12505	08.11.2012	710448	3504543	596.7	254.15	7.5	431	21.0	491	14.7	27.6	1.41 ± 0.07	1.7 ± 0.2	0.73 ± 0.05	0.1 ± 0.05	1.0 ± 0.2	1.2 ± 0.3	4.4			5.6	
8	Al-Rihya	13515	24.05.2013	697253	3482073	698.2		7.3	352	25.5	599	4.71	44.1	0.17 ± 0.02										
Wells - recharge zone (Albin)																								
2	Jenaisk 1	13487	10.02.2013	708126	3515719	701.0	120.9	7.3	280	20.4	679	19.5	64.3	8.91 ± 0.40					1.7 ± 0.3	148.5	5.6	13.0	188.8	
	Jenaisk 1	13505	23.05.2013	708126	3515719			7.2	305	20.6	682	25.2	67.4							4.4				
Wells - transition zone (Albin)																								
3	Al-Azra 3	12507	09.11.2012	715119	3514801	497.6		7.3	424	24.1	607	21.6	45.0	0.96 ± 0.06	ca. 180	5.2 ± 0.3	0.9 ± 0.1	2.9 ± 0.3	<0.5	2.2			62.3	
	Al-Azra 3	12511	24.05.2013	715119	3514801			7.3	335	25.0	569	16	36.8							1.7			7.5	
4	PWA 3	13513	24.05.2013	710746	3505529	629.5		7.4	348	24.6	514	7.95	22.7	0.49 ± 0.03						1.5			6.5	
6	Hendon 4	13510	23.05.2013	709107	3500349	774.0	458.9	7.2	350	24.1	548	4.86	23.2	0.32 ± 0.03						5.5			66.1	
7	Bani Naim 2	12510	09.11.2012	709445	3488704	540.5	453.5	7.3	415	26.7	551	5.64	22.7	0.19 ± 0.02	0.02 ± 0.05	<0.01	<0.01	0.5 ± 0.1	<0.5	0.4				
Wells - transition zone (Cenomanian)																								
10	Mizpe Jericho 2	12518	12.11.2012	727516	3520886	-19.8	328.71	7.3	509	24.5	758	43.3	74.4	0.80 ± 0.05	25 ± 5	2.7 ± 0.2	4 ± 1	0.1 ± 0.1	1.4 ± 0.3	1.4			3.3	
	Mizpe Jericho 2	12520	28.05.2013	727516	3520886			7.2	377	24.7	761	42.7	73.5							9.2			22.1	
Springs - transition zone N (Cenomanian)																								
9	Ein Ajja	13470	04.02.2013	725617	3536000	32.0		7.2	387	20.9	618	21	39.0	0.64 ± 0.04					2.9 ± 0.3	25.7			6.4	
	Ein Ajja	13518	27.05.2013	725617	3536000			7.2	500	21.3	561	15.9	34.5										33.3	11.8
Springs - transition zone S (Cenomanian)																								
11	Augot uppermost	12341	27.10.2012	723684	3483288	-152.9		7.3	413	27.3	835	19	117.0		2.6 ± 0.3	1.4 ± 0.1	0.21 ± 0.05	1.8 ± 0.2	0.5 ± 0.3	0.4			1.3	
Wells - discharge zone (Cenomanian)																								
12	Jericho 2	13479	07.02.2013	729844	3526155	-168.6	328.71	7.1	290	24.7	1307	12.9	234	0.20 ± 0.02					2.0 ± 0.3	73.0			4.4	
	Jericho 2	13522	28.05.2013	729844	3526155			7.0	295	25.1	1895	<46	381							129.3			135.6	
Wells - discharge zone (Albin)																								
13	Jericho 4	13523	28.05.2013	728379	3531816	-115.5	386.39	7.2	335	27.3	1067	6.6	208	0.15 ± 0.01					<0.6 (0.307)	7.2			56.4	
14	Jericho 5	13524	28.05.2013	727200	3533467	-44.8	456.6	7.1	339	25.1	1369	<46	224	0.10 ± 0.02					<0.5 (0.307)	6.2			14.3	
Wells - discharge zone (Quaternary)																								
15	Arab Project 19-1470 (Arab 70)	13497	16.02.2013	736108	3527441	-306.7		6.9	308	26.3	4860	22.2	1303	0.24 ± 0.03					0.4 ± 0.3	0.3			2.0	
	Arab Project 19-1470 (Arab 70)	13526	01.06.2013	736108	3527441			6.9	357	26.2	4300	<46	1202										12.9	
16	Arab Project 19-1472 (Arab 72)	13498	16.02.2013	736124	3527575	-306.8		7.3	246	26.6	3300	22.6	926	0.26 ± 0.04						3.4			1.2	
	Arab Project 19-1472 (Arab 72)	13527	01.06.2013	736124	3527575			7.1	291	27.0	4040	<46	1086							2.8			7.8	
17	19-13/024A	13500	16.02.2013	735921	3525245			7.3	463	24.8	1527	10.7	234	0.23 ± 0.02					<0.6	0.7			0.5	
Springs - discharge zone (Quaternary)																								
18	Ein Feshkha - A	12534	01.11.2012	732218	3510111			7.3	337	26.3	12620	1.54	4428	0.11 ± 0.02					0.9 ± 0.3				35.7	
19	Ein Feshkha - B	12535	01.11.2012	732412	3509538			7.8	364	26.8	5860	8.18	1935	0.10 ± 0.01					0.7 ± 0.3					
20	Ein Feshkha - C	13488	11.02.2013	732195	3509480			6.9	520	27.6	4680	4.13	1536	0.13 ± 0.02					0.8 ± 0.3	0.3				
	Ein Feshkha - C	13531	07.06.2013	732195	3509480			7.0	534	27.5	4670	<46	1381										11.3	
21	Ein Feshkha - D	13478	06.02.2013	733432	3510612			7.5	107	24.6	4230	<23	1326	0.15 ± 0.03					0.8 ± 0.3	0.3			40.0	
	Ein Feshkha - D	13502	22.05.2013	733432	3510612			7.8	244	26.5	4250	<46	1694	0.15 ± 0.03									12.5	
22	Ein Feshkha - Einot Zukim 1+2	12536	02.11.2012	732201	3511443			6.8	418	29.2	3650	20.45	1112	0.15 ± 0.02					1.0 ± 0.3				170.3	
	Ein Feshkha - Einot Zukim 1+2	13474	05.02.2013	732201	3511443			7.2	444	25.2	3520	9.02	1098	0.10 ± 0.02					0.7 ± 0.3	0.4				
	Ein Feshkha - Einot Zukim 1+2	13532	07.06.2013	732201	3511443			7.2	392	28.1	3720	<46	985										29.9	
Precipitation																								
23	precipitation Jerusalem	14517	24.11.2014	709690	3519284			6.2				6.4		0.13 ± 0.02										
	precipitation Jerusalem	14518	26.11.2014	709690	3519284			6.1				21.4		0.30 ± 0.03										
	precipitation Jerusalem	14519	15.12.2014	709690	3519284			6.5				5.0		0.85 ± 0.04										
	precipitation Jerusalem	14520	13.12.2014	709690	3519284			6.3				10.1		0.26 ± 0.02										
	precipitation Jerusalem	14521	04.01.2014	709690	3519284			6.1				10.3		0.21 ± 0.02										
	precipitation Jerusalem	14522	08.01.2014	709690	3519284			6.3				29.5		0.18 ± 0.02										
Pore water from Dead Sea sediments																								
24	Pore water A	13600	21.11.2013	733170	3510300			5.4				14754		1.16										
	Pore water A	13601	21.11.2013	733170	3510300			5.4				237441		1.08										
	Pore water B	13602	21.11.2013	733170	3510300			5.4				236248		1.41										



2.3.1 Parameterization and model setup of LUMPY

To parameterize the unsaturated (vadose) zone in the recharge area, characteristic wells (Samia 2 and Herodion 1) were used (Tab. 2).

Table. 2 Summary of DM, PM and PEM parameters for the wells Samia 2 and Herodion 1. Schematic graphs illustrate parameters and their individual levels in [m asl.] along both boreholes; water-filled (saturated) part of the aquifer is indicated by blue colour, screen section by checked pattern, aquitard by stripe pattern, respectively.

	<i>Samia 2 well</i>		<i>Herodion 1 well</i>	
Surface Elevation [m msl.]	420		570	
Groundwater level [m msl.]	220		330	
Start Filter section [m msl.]	245		316	
End Filter section [m msl.]	174		237	
Aquifer base [m msl.]	150		220	
<i>LUMPY parameters</i>				
Distance of screen top below water table	0		14	
Z1 [m]				
Distance of screen bottom below water table	46		93	
Z2 [m]				
Saturated aquifer thickness				
L [m]	70		110	

Influence of a thick unsaturated zone. Gas tracers like CFCs and SF₆ predominantly pass the unsaturated (vadose) in the gas phase, posing certain problems for their interpretation. In unsaturated zones of less than 5m thickness, the gas composition of soil air resembles that of the atmosphere (Cook & Solomon 1995; Engesgaard et al., 2004). However, a time lag may occur for the diffusive transport of CFCs and SF₆ through thick unsaturated zones of porous aquifers (Cook & Solomon 1995). This time lag is a function of the tracer diffusion coefficients, tracer solubility in water, and moisture content (Weeks et al., 1982; Cook and Solomon, 1995). An occurring time lag always results in a gas tracer age older than the time of groundwater recharge. In fractured (or karstic) aquifers, however, the time lag may be much shorter (e.g. Darling et al., 2005) resulting in ages of CFC's or SF₆ obtained from groundwater, which effectively represent residence time of groundwater since recharge approached the groundwater table, without a time lag and as if the tracer were transported within the saturated zone only.



The present study aims to estimate travel times in the thick unsaturated zone (Cook and Solomon, 1995; Plummer et al.,
245 2006), by estimating the time lag as the relative difference in mean residence time between gas and water-bound tracers,
applying both, water-bound tracers (^3H , ^{36}Cl) and gas tracers (CFCs, SF_6). Particularly, the wells Samia 2 and Herodion 1 of
the Upper Cenomanian are selected in order to consider wells close to the recharge area with a thick unsaturated zone of 200-
240 m (Table 2). They are in the eastern part of the recharge zone (Fig. 1), where the limestone is intensely fissured
vertically and partly karstified.

250 2.3.2 Well construction, aquifer data and calculation of recharge rates

The convolution integral of the partial exponential model (PEM) can be further constrained by the well construction data like
(saturated) depth to the top of the screen, the screen length and saturated aquifer thickness (Jurgens et al., 2016). This data
was taken from the construction logs of the investigated production wells (Tab. 2).

Based on the estimated MRT of the applied lumped parameter models DM, PM and PEM, recharge rates can be estimated.
255 However, the formulas to apply differ slightly between the different models. The following Equation (4) allows calculating
the recharge rate R for the PEM (Jurgens et al., 2016; Vogel, 1967):

$$R = \frac{\phi \cdot L}{MRT} \quad (4)$$

where ϕ is the porosity of the aquifer, L is the saturated aquifer thickness and the MRT is valid for the whole aquifer (which
is an output in LUMPY derived from the fitted MRT for the sample and using the well parameters $Z1$, $Z2$ and L in Table 2).

260 As for the DM and PM, L is the distance from the groundwater surface to the depth of the centre of the screened section of
the well. As for the DM, not the MRT (the mean residence time of the sample) but the *peak time* is used, which is also an
output of LUMPY, being calculated applying Equation (5) (Suckow, 2014b):

$$Peak\ Time = \frac{MRT}{P_e} \left(\sqrt{9 + P_e^2} - 3 \right) \quad (5)$$

Depth to centre of the water-filled screen section from groundwater level is 23 m for Samia 2 and 53.5 m for Herodion 1
265 (Table 2).

Tracer transport in karst areas is influenced by double porosity effects, particularly a retardation of the tracer can be assumed
due to diffusive loss into the adjacent limestone of the fissures. A correction of calculated MRTs and recharge rates may be
possible applying a retardation factor (Equation 6) (Maloszewski et al., 2004; Purtschert et al., 2013);

$$Retardation = \frac{\phi_{tot}}{\phi_{eff}} \quad (6)$$

270 where ϕ_{tot} is the total porosity and ϕ_{eff} is the effective porosity. An assumed porosity in the carbonate karst aquifers may
vary between <2% (representing the open fissures and solution pipes) to 20% (total pore space in the aquifer rock).

Groundwater recharge was also estimated using the chloride mass balance method, which was successfully applied
elsewhere (Allison and Hughes, 1978; Crosbie et al., 2018; Eriksson and Khunakasem, 1969; Purtschert et al., 2013; Wood



and Sanford, 1995) and which assumes Cl-input to groundwater originates from Cl-concentration in precipitation, which becomes enriched due to evaporation only (Eq. 7):

$$R_{CMB} = \frac{P \cdot Cl_P}{Cl_{GW}} \quad (7)$$

The formula consists of the mean annual precipitation P and the chloride concentrations in precipitation Cl_P and groundwater Cl_{GW} in [mg/l]. The mean annual precipitation in the recharge area is about 550 mm. The average long-term Cl-content in rain water is ca. 5 mg/l (Herut et al., 1992), while it reaches 28 mg/l and 35-38 mg/l in groundwaters of wells Herodion 1 and Samia 2, respectively.

3 Results

The $^{36}\text{Cl}/\text{Cl}$ ratios in precipitation, which falls in the recharge area, are assumed to be stable since the 1980s, as indicated by rainwater samples collected during winter 2014/2015, which show $^{36}\text{Cl}/\text{Cl}$ ratios of 1.3×10^{-14} to 5.5×10^{-14} , resembling results from the early 1980s (Herut et al., 1992). Contrastingly, tritium concentration in precipitation continuously declined to about 4-6 TU today (IAEA/WMO, 2017). Well-fitting the hydrogeological trichotomy of the study area, analytical results (Table 2) resemble the regional situation and group according to the individual aquifers (Fig. 3).

Recharge area. In wells Samia 2 and Herodion 1, representative for the recharge area of the Upper Cenomanian aquifer, tritium concentrations of 2.1 TU and 1.2 TU as well as $^{36}\text{Cl}/\text{Cl}$ of 1.41×10^{-13} and 1.57×10^{-13} , respectively, are observable. Further south, in well Al Reehiya, groundwater in the aquifer show lower $^{36}\text{Cl}/\text{Cl}$ and ^3H of 1.73×10^{-14} and <0.5 TU, respectively. The gas tracer concentration in that part of the aquifer is low, but detectable and showed $\text{SF}_6 = 1 \pm 0.2$ fmol/l, CFC-12 = 1.2 ± 0.1 pmol/l, CFC-11 = 2.3 ± 0.3 and CFC-113 = 0.19 ± 0.05 in Samia 2 and comparable values in Herodion 1 (Table 1). Well Jerusalem 1, which represents the Lower Cenomanian aquifer extract groundwater showing as low ^3H concentrations (1.7 TU) as observable in the Upper aquifer, but much higher $^{36}\text{Cl}/\text{Cl}$ (8.9×10^{-13}).

Transition zone. Groundwater, emerging from the perched Turonian aquifer (Ein Auja) and from the Upper Cenomanian aquifer (Mizpe Jericho 2) show low $^{36}\text{Cl}/\text{Cl}$ ratio of 6.35×10^{-14} and 7.99×10^{-14} and ^3H concentrations of 2.9 TU and 1.4 TU, respectively. Well Mizpe Jericho 2 stands out due to its high CFC contents, reaching values of CFC-11 = 25 pmol/l and CFC-113 = 4 pmol/l, higher than possible in equilibrium with the atmosphere (4.5 pmol/l and 0.5 pmol/l respectively). Further south, the Arugot spring discharges 300 m above the Dead Sea from the Upper Cenomanian aquifer, closely to the brim of the graben flank but still within the Arugot valley and hence within the transition zone. The emerging groundwater is high in SF_6 (2.1 fmol/l), CFC-11 (3.8 pmol/l) and CFC-12 (1.8 pmol/l) but contains very low ^3H (0.5 TU), suggesting a well-developed karst network which allows sufficient gas exchange of an older groundwater with recent atmosphere along its flow path.

Groundwater in the Albian aquifer (wells PWA 3, Herodion 4, Bani Naim 3) is low concentrated regarding CFCs, SF_6 , and ^3H (<1 TU) and shows low $^{36}\text{Cl}/\text{Cl}$ ratios of $1.9\text{--}4.9 \times 10^{-14}$. An exception is well Azaria 3, at the edge between recharge and transition zone, which shows higher $^{36}\text{Cl}/\text{Cl}$ (9.59×10^{-14}) than recent precipitation, much less tritium (0.5 TU) and high



concentrations of CFC-12 (5.2 pmol/l), which are again, well above values in equilibrium with the atmosphere (max 2.3 pmol/l).

Discharge area. Groundwater from the Upper Cenomanian aquifer (Jericho 2) show similar low $^{36}\text{Cl}/\text{Cl}$ ratios of 2.04×10^{-14} and 2 TU similar to groundwater upstream in the transition zone. In groundwaters pumped in Jericho 4 and 5 from the
 310 Albian aquifer, $^{36}\text{Cl}/\text{Cl}$ and ^3H contents are even lower: $1.03\text{-}1.15 \times 10^{-14}$ and <0.6 TU, respectively. These low $^{36}\text{Cl}/\text{Cl}$ might result from admixing brines, which are abundant within the rift. It becomes evident in groundwater of Ein Feshkha, where interstitial brines ($^{36}\text{Cl}/\text{Cl} = 1.08 \times 10^{-14}$) hosted in the interstitial space of the Quaternary sediment, get leached by approaching fresh groundwaters and cause lowest observable $^{36}\text{Cl}/\text{Cl}$ of $1.01\text{-}1.51 \times 10^{-14}$.

Brackish groundwaters from the Arab wells 19-13/24A, 19-14/70 and 19-14/72, which are drilled east of Jericho and well
 315 within in the graben, show $^{36}\text{Cl}/\text{Cl}$ of $2.29\text{-}2.57 \times 10^{-14}$ being higher than the ratios in (i) fresh groundwaters from both Cretaceous aquifers (Jericho 2, 4, 5) and (ii) in Ein Feshkha and hence, refer to a different source of salinization.

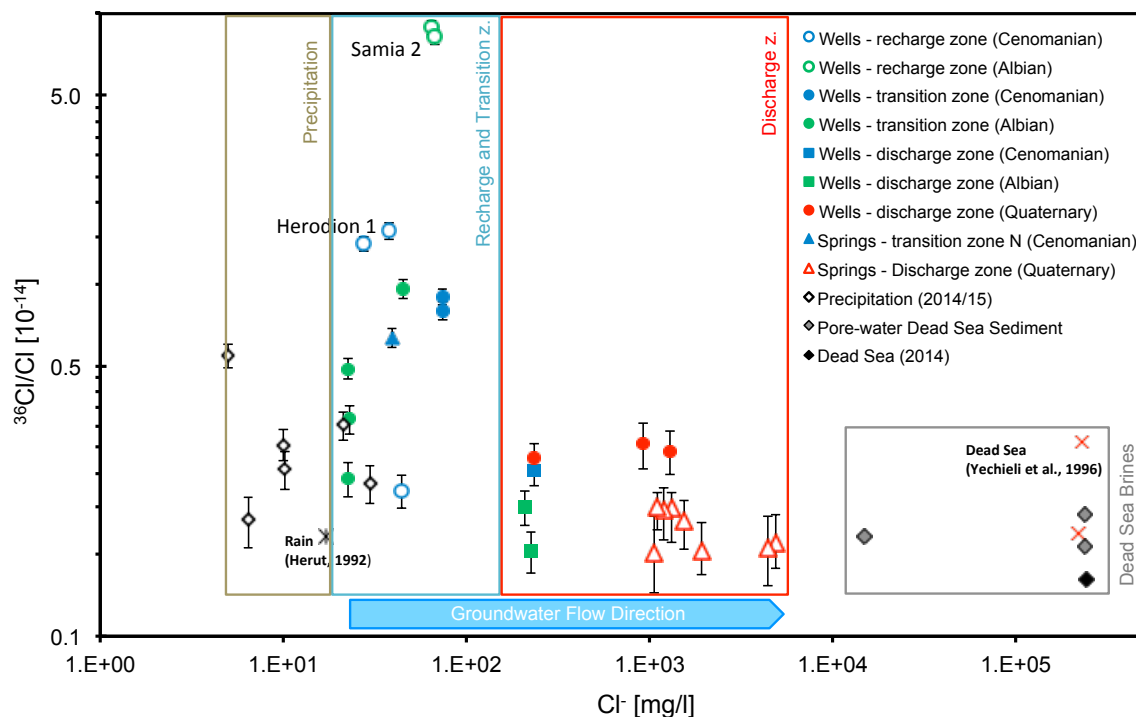


Figure 3: Results of $^{36}\text{Cl}/\text{Cl}$ versus chloride concentrations in the investigation area in log scale.

In general, the following patterns can be extracted from the hydrochemical and tracer data:

- (i) spring water of the Upper Cenomanian (Ein Auja) contains groundwater infiltrated after the era of atmospheric bomb testing, indicated by tritium and $^{36}\text{Cl}/\text{Cl}$ comparable with recent rain water;



- 320 (ii) groundwater of the Upper Cenomanian close to the recharge area shows $^{36}\text{Cl}/\text{Cl}$ ratios higher than recent rain
combined with low tritium contents, possibly referring to admixtures of water from the early fission bomb
testing but before thermonuclear devices;
- (iii) along the flow path and in the lower aquifer $^{36}\text{Cl}/\text{Cl}$ is shifted to lower ratios due to admixture of saline water,
the endmember being brine similar to the Dead Sea probably admixed as pore water from earlier higher sea-
325 levels;
- (iv) the lower aquifer shows detectable admixtures of young water only in the vicinity of Jerusalem and Bethlehem,
demonstrated by tritium and $^{36}\text{Cl}/\text{Cl}$;
- (v) springs in the south (Ein Feshkha and Arugot) are free of tritium and show background $^{36}\text{Cl}/\text{Cl}$ ratios indicating
no recent recharge, although SF_6 and CFCs are high - recent gas exchange in karst structures may have reset the
330 SF_6 and CFC “clocks”.

Anthropogenic organic trace substances Simazine, NAP und ACE-K are detectable in trace concentrations in nearly all
sampled wells of the upper and lower aquifer (Fig. 4), indicating input younger than 40 years. Combining NO_3 contents with
concentrations of herbicide Simazine in the sampled groundwaters allow to distinguish between the origin of NO_3 , either
from domestic waste water or from agriculture (Fig. 4a). All groundwaters show positive correlations between nitrate and
335 Simazine, while there is no clear systematic trend observable, being specific for one of the aquifers nor a specific region.
Embracing the samples according to aquifers suggests, groundwater in the Upper Cenomanian aquifer is stronger influenced
by waste water inflow than groundwaters in the Albian aquifer. Groundwater from Mizpe Jericho 2, with high NO_3 (43 mg/l)
at comparable low Simazine concentrations clearly underline the contribution of waste water. Contrastingly, groundwaters
from Jericho 2 and Jerusalem 1 may refer to a higher contribution from agriculture.

340 Looking at ACE-K and NAP as pure waste-water indicators (Fig. 4b), two distinctly opposite trends are distinguishable.
Trend 1 is characterized by very low NAP concentrations and high concentrations of ACE-K as observable in wells Jericho 4
(56 ng/l) and Jericho 2 (136 ng/l). The opposite trend is found in Ein Feshkha spring D, Jerusalem 1 and Samia 2, shows
high NAP concentrations (170, 168 and 137 ng/l, respectively) at low ACE-K concentrations (<20 ng/l). If one excludes Ein
Feshkha, NAP concentrations decrease from recharge area (Jerusalem 1, Samia 2) to the discharge area (Jericho 2 and 4),
345 most probably due to adsorption onto the aquifer matrix along the flow path. As for Ein Feshkha D, the NAP contamination
here is comparable high as in the recharge area and much larger than the NAP contents in Ein Feshkha C and Enot Zukim.
This suggests a significantly shorter residence time of the contaminant in the aquifer, which requires a source much closer to
the spring, probably a leakage in the TWW-pipeline, passing the area just upstream the spring. The only groundwater
without any anthropogenic contamination is Arugot spring.



350 4 Discussion

The patterns observed for the different measured substances deliver a heterogenous picture of the study area. Starting at the top, a shallow perched aquifer system with short residence times is indicated for the Ein Auja spring based on high $^{36}\text{Cl}/\text{Cl}$ ratio (6.35×10^{-14}), tritium content (2.9 TU) and low mineralisation like recent precipitation.

355 In the recharge area of the Cenomanian and Albian aquifers, clear indications for a contribution of recharge enriched with ^{36}Cl from nuclear bomb tests is observable in freshwater wells (Cl-content <67 mg/l) Jerusalem 1, Herodion 1 and Samia 2, which show $^{36}\text{Cl}/\text{Cl}$ of $1.4\text{--}8.9 \times 10^{-13}$, being much larger than in precipitation from after 1980 ($^{36}\text{Cl}/\text{Cl} = <5.5 \times 10^{-14}$). Furthermore, gas tracer results in Herodion 1 and Samia 2 imply, the aquifer contains groundwater recharged after 1960. Organic pollutants concretize it even more. High Simazine contents in Jerusalem 1 and high loads of NAP in Samia 2 and Jerusalem 1 indicate significant contamination through a young water fraction in both aquifers, the Upper Cenomanian and
360 the Albian.

Within the transition zone, wells Al Azaria 3 (Albian) and Mizpe Jericho 2 (Upper Cenomanian) show $^{36}\text{Cl}/\text{Cl}$ still larger than in precipitation from the last four decades, indicating at least similar or even older recharge periods than of groundwater in the recharge zone. However, high concentrations of CFC-11 and of ACE-K in Mizpe Jericho 2 and high concentrations of CFC-12 and NAP in Al Zaria 3 also show a significant contribution of young water fraction to these wells. Contrastingly,
365 anthropogenic gas tracers are close to or even below the limit of detection in groundwater samples from Albian aquifer at wells PWA 3, Herodion 4 and Bani Naim 3, indicating no fresh water input from the last decades and travel times longer than 70 years. A similar figure results from taking these three wells and forming a N-S transect through the Albian aquifer in the mountain range: their low $^{36}\text{Cl}/\text{Cl}$ ratios, which are well within the range of recent precipitation, decrease from north to south while chloride remains stable. Since ^3H contents are below limit of detection (<0.5 TU), the observed groundwaters are
370 considered to be mainly pre-bomb water and hence older than 6-7 decades.

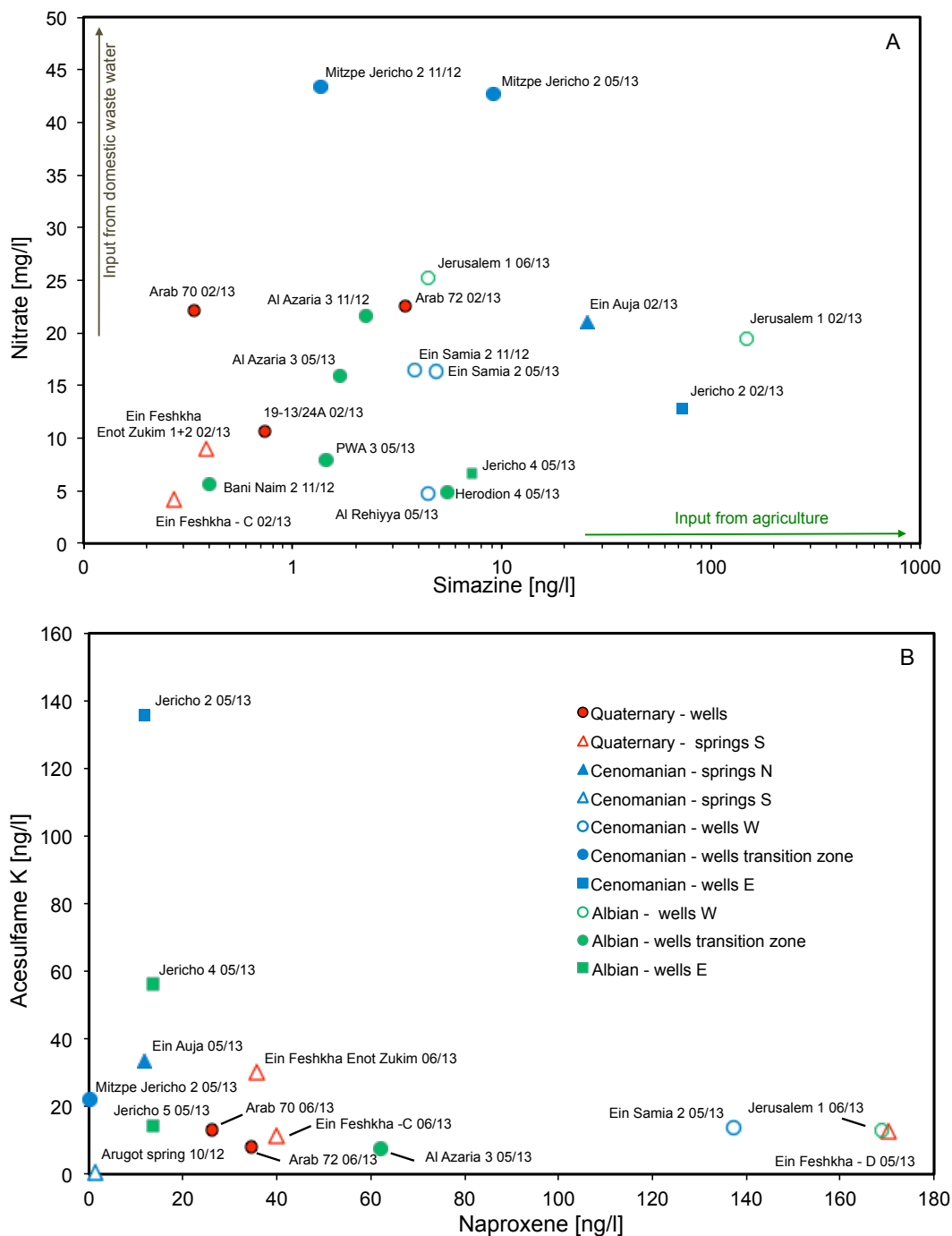


Figure 4: showing cross plots of (A) NO₃ and Simazine in sampled waters, suggesting different sources of both pollutants; the blue and green lines bracket respectively coloured spaces and indicate the fields, in which samples from Upper Cenomanian and Albian aquifer plot; and (B) Acesulfame K and Naproxene as indicators for waste water (treated and untreated) in the sampled waters. Legend for both figures is given in (B).



In the southern part of the study area, survey stations are even rarer. However, Well Al Rehiya shows very low $^{36}\text{Cl}/\text{Cl}$ and low ^3H , indicating either unmixed pre-bomb water or dilution of recent precipitation with much older water possibly originating from aquifer parts even further southwards. The latter is promoted by results from numerical flow modelling, which indicate an SW-NE directed upstream flow (Gräbe et al., 2012). Negligible concentrations of NAP, ACE-K and Simazine in Arugot spring water, which emerges at the furthest end of the southern transition zone, show no anthropogenic contamination by wastewater. This leads to the assumption that open karst-conduits allow efficient exchange with the atmosphere along the subsurface flow of the spring water, resulting in CFC-11 and CFC-12 contents, in equilibrium with the atmosphere.

Groundwaters from Albian (Jericho wells 4 and 5) and from Upper Cenomanian (Jericho 2) in the discharge area are characterized by $^{36}\text{Cl}/\text{Cl} < 2 \times 10^{-14}$. While the formers are free of tritium, Jericho 2 shows 2 TU, indicating at least a fraction of younger water. Since well Jericho 2 is drilled directly at the mouth of the Qilt Valley, we assume, the young water fraction may reach the well through rapid infiltration through fractures and karst conduits within the Valley. The young water fraction in Jericho 2 is also proven by high Simazine and ACE-K concentration in the groundwater of that well.

Low $^{36}\text{Cl}/\text{Cl}$ ratios in the wells drilled into the Quaternary section east of Jericho (ca. 2×10^{-14}) and in the Ein Feshkha springs (ca. 1×10^{-14}) refer to enrichment of fresh groundwater with different sources of salinity, showing low $^{36}\text{Cl}/\text{Cl}$ ratios. The brackish wells East of Jericho are known to draw groundwater from the Upper Cenomanian aquifer (Khayat et al., 2006a), which passes the graben fault and enters into the sediment body, where it may leach abundant evaporitic minerals. It also contains water from agricultural irrigation and waste water as confirmed by high NO_3 concentrations, the presence of Simazine and occasionally remarkable ACE-K contents.

Contrastingly, Dead Sea brines, which get released from the sedimentary body, mix in Ein Feshkha with approaching fresh groundwaters from the Graben shoulder. The low ^3H (< 1 TU) in Ein Feshkha indicate the age of the admixing Dead Sea brine to be before 1960. During that time, lake level was at -390 m asl. and higher (Hassan and Klein, 2002). At the time, Dead Sea brine infiltrated into the shallow lake bed, where nowadays the observed springs emerge, at an elevation of -392 to -395 m asl. However, Ein Feshkha springs C, D and Enot Zukim receive young water fractions, since NAP and ACE-K contents in the former are as high as in groundwater in the recharge zone (Jerusalem 1) and in the latter at least enhanced.

The next section will exemplify a more detailed modelling of mean residence times with transient tracers where the data allows this approach. This was possible only on two wells. Wells of the Albian aquifer in the transition zone are not interpreted using LPM due to contaminations with CFCs (e.g. Al Azaria 3, Table 1) or very low concentrations of the anthropogenic gases (e.g. Bani Naim 3). If the measured concentrations of the anthropogenic trace gases CFCs and SF_6 are much higher than expected from solubility equilibrium with the atmosphere this is regarded as contamination (e.g. Mizpe Jericho 2). The tritium concentrations of 1.5 TU and 2 TU in Mizpe Jericho 2 and Jericho 2, respectively, indicate a reasonable fraction of recent rain. Due to the continuous outflow of the springs along the coastline and chemical mixing patterns of the spring water, it is assumed that there is also a connection to the water resources of the Lower Cretaceous aquifer, which could provide water with longer residence times. All springs in the discharge area (e.g. Ein Feshkha) have



less than 0.5 TU and $^{36}\text{Cl}/\text{Cl} < 1.5 \cdot 10^{-14}$. However, the organic tracers ACE-K, Simazine and NAP are detectable also in these springs. Their values in Ein Feshkha are between 5 to 30 times above the detection limit (Table 1 and section 2.2). Since the input function of the organic tracers cannot be quantified, the fraction of young water, representing that concentration cannot
410 be calculated. This discrepancy (no tritium, no anthropogenic ^{36}Cl , but organic tracers) can be understood by quantifying the detection limit of “young water” that tritium allows: recent rain in the area has 4 TU, so a value of < 0.5 TU is equivalent to less than 12% recent rain. This implies the young end member in the mixture must have a concentration of ACE-K, Simazine® and NAP > 10 times higher than measured in the groundwater samples. A more precise quantification of the young water fraction in these springs is only possible with either a lower detection limit for tritium (e.g. determination of ^3H
415 via ingrowth with detection limit 0.005 TU (Bayer et al., 1989; Beyerle et al., 2000; Sültenfuss et al., 2009) or a precise quantification of the input of ACE-K, Simazine® and NAP. Both is beyond the scope of the present study.

4.1 Lumped parameter modelling: delay of gas tracer in the unsaturated zone

Detailed lumped parameter modelling of tritium, $^{36}\text{Cl}/\text{Cl}$ and the gas tracers was performed only for the wells Samia 2 and Herodion 1 since only for these there is a consistent data set for all tracers (Table 1). Earlier interpretation of groundwater
420 hydraulics based on groundwater level measurements determined a very fast transfer velocity of the water phase through karst holes to the groundwater table (Jabreen et al., 2018). LPM was therefore done in several steps: first a mean residence time in agreement with measured values for tritium and the bomb-spike of $^{36}\text{Cl}/\text{Cl}$ was derived. Then a delay for the gas tracer CFCs and SF_6 was derived assuming a simple piston flow transport to describe the residence time of these tracers in the unsaturated zone. Once the delay created an agreement between the water – bound tracer tritium and $^{36}\text{Cl}/\text{Cl}$ with the gas
425 tracer CFC-11, CFC-12, CFC-113 and SF_6 , the mean residence time in the saturated zone was investigated using the PM, DM and PEM to describe flow in the saturated zone. From the MRT in the saturated zone, groundwater recharge was estimated in a final step and compared with results from the CMB method and earlier numerical groundwater models.

Results for tritium and $^{36}\text{Cl}/\text{Cl}$ fit to a MRT of about 10a in the saturated zone using the PM, the dispersion model results in 20a MRT and for the partial exponential model 20a and 16a MRT are estimated (Table 4). These estimated MRT of the
430 water-bound tracers then allowed for determining the gas delay in the unsaturated zone. For every applied model (PM, PEM and DM) the gas delay is estimated using the calculated model curve of the water-bound tracers and using the delay as parameter to fit the gas tracer measurements of Samia 2 and Herodion 1. This resulted in specific gas delays for every concentration of the CFC's and SF_6 , exemplified for CFC-12 in Figure 5 and provided for all gas tracers in Table 3.

for all gas tracers in Table 3.

435 Estimates for every model result in different gas delays related to the MRT of water-bound tracers in the wells Samia 2 and Herodion 1 (Table 3). The delays of the CFC's are comparable to each other and differ from 14 to 24 years for Samia 2 (Figure 5) and from 14 to 30 years for Herodion 1 over all calculated models. The gas delay in Samia 2 is lower than in Herodion 1, which is reasonable regarding the thicker unsaturated zone in Herodion 1 (Table 2). Ideally the transport of gas tracers in the subsurface would result in similar delays for all gas tracers (Cook and Solomon, 1995). The delay determined



440 for SF₆ was significantly lower than for the CFC's (Table 3) indicating higher concentrations of SF₆ as compared to the expectation from the CFC model results. This could be a result of biological degradation of the CFC's in the upper part of the unsaturated karst zone, or from considerable excess air, which influences SF₆ much more than the CFCs. A decision between these two processes is possible determining excess air independently measuring the concentrations of all noble gases, which were not available in the present study.

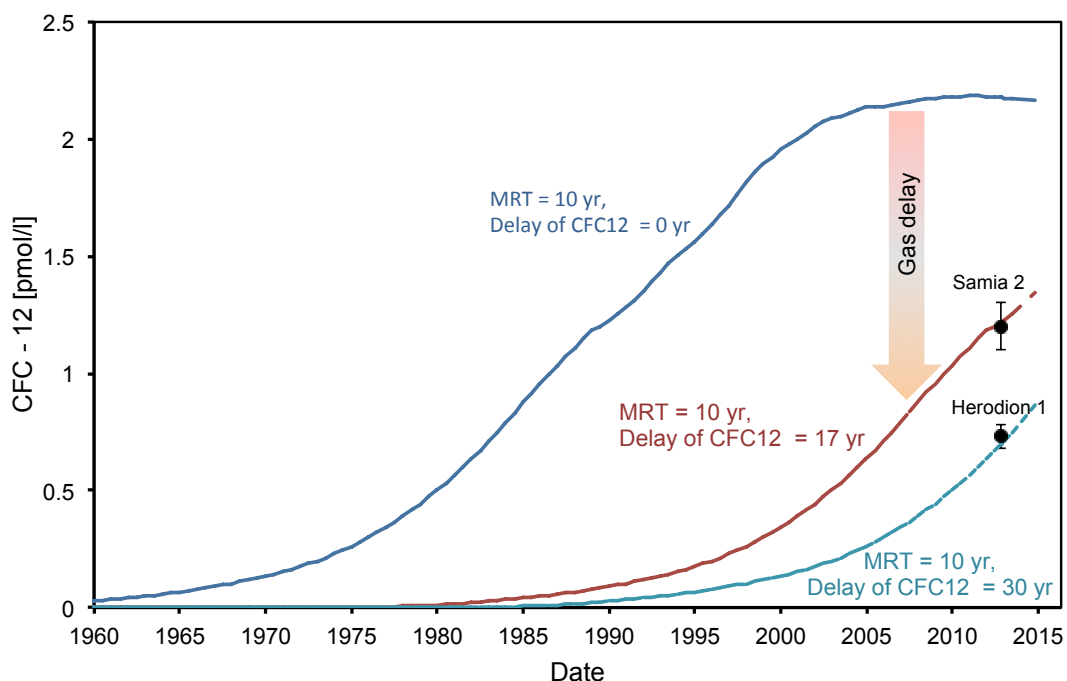


Figure 5: In a CFC-12 vs. time plot, a piston flow model with MRT of 10 years obtained from the water-bound tracer tritium and ³⁶Cl/Cl fits the CFC-12 measurements with a gas delay of 17 years for Samia 2 and 30 years for Herodion 1.

445

Table 3. Summary of gas delay in the unsaturated zone for each gas tracer and the different models. PM = piston flow model, DM = dispersion model, PEM = partial exponential model. For the parameters of the PEM see Table 2.

Model	PM		DM		PEM	
	Samia 2	Herodion 1	Samia 2	Herodion 1	Samia 2	Herodion 1
CFC-11	24	28	14	18	20	25
CFC-12	17	30	14	20	20	28
CFC-113	23	22	9	14	17	22
SF ₆	8	8	0	0	7	6



4.2 Lumped parameter modelling: mean residence times in the saturated zone

450 In the next step, the determined gas delays of the gas tracers (Table 3) in the unsaturated zone were used to estimate the
 MRT of the water-bound tracers and the gas tracers in the saturated zone. Only the gas delay allowed a fit to the
 measurement combination of the gas tracer concentrations and the water tracer results of Samia 2 in the time range of 10 to
 15 years MRT for the piston flow model, 17 to 28 years MRT for the dispersion model and 26 to 46 years for the partial
 exponential model (Table 4). Comparing the different model approaches, estimates of the saturated MRT systematically
 455 increase in the sequence PM-DM-PEM in both wells, which is a result of the increasing amount of dispersion and mixing in
 these models.

In contrast to Samia 2, it was not possible to fit the results of Herodion 1 without an admixture of tracer-free old water. With
 and without delay the lumped parameter curves do not fit the measurements of the lower tritium concentration in Herodion 1
 (1.2 TU) whereas they do for Samia 2. The well Herodion 1 is situated in the recharge zone, but also in the lower part of the
 460 Upper Cenomanian aquifer. The model results therefore indicate an admixture of at least one older water component
 ascending from the Albian aquifer and diluting the younger tritium concentrations. This can be described with a two-
 endmember mixing line, which fits the tritium measurement of Herodion 1 (Figure 6).

Table 4 Summary of modelled MRTs of Samia 2 and Herodion 1 extracted from different tracer combinations. PM = piston
 flow model, DM = dispersion model, PEM = partial exponential model.
 465 *estimated fit.

Sampled well	Samia 2			Herodion 1		
	PEM	DM	PM	PEM	DM	PM
CFC-11 vs CFC-113	31 – 44	20 - 23	10 - 14	17 - 22	no fit	11 - 13
CFC-11 vs. SF ₆	31 – 44	21 - 25	9 - 13	21 - 23	17 - 22	10 - 12
CFC-12 vs. SF ₆	38 – 46	21 - 23	10 - 13	18 - 20	22 - 24	10 - 11
³⁶ Cl/Cl vs. SF ₆	36 – 37	20 - 22	9 – 15*	17 - 18	19 - 20	9 - 15
³⁶ Cl/Cl vs. CFC-113	36 – 38	21 - 22	11 – 15*	16 - 28	no fit	9 - 18
³⁶ Cl/Cl vs. CFC-12	36 – 38	21 - 23	11 – 14*	17 - 18	20 - 21	11 - 12
³⁶ Cl/Cl vs. Tritium	36 – 38*	20 - 22	9 - 29	Mixing ratios of 3:7 to 4:6 (1 yr MRT and 170 yrs MRT)		
Tritium vs. SF ₆	26 – 44	18 - 23	10 - 15	Mixing ratios of 3:7 to 4:6 (1 yr MRT and 170 yrs MRT)		
Tritium vs. CFC-12	38 – 45*	21 - 23	10 - 14	Mixing ratios of 3:7 to 4:6 (1 yr MRT and 170 yrs MRT)		

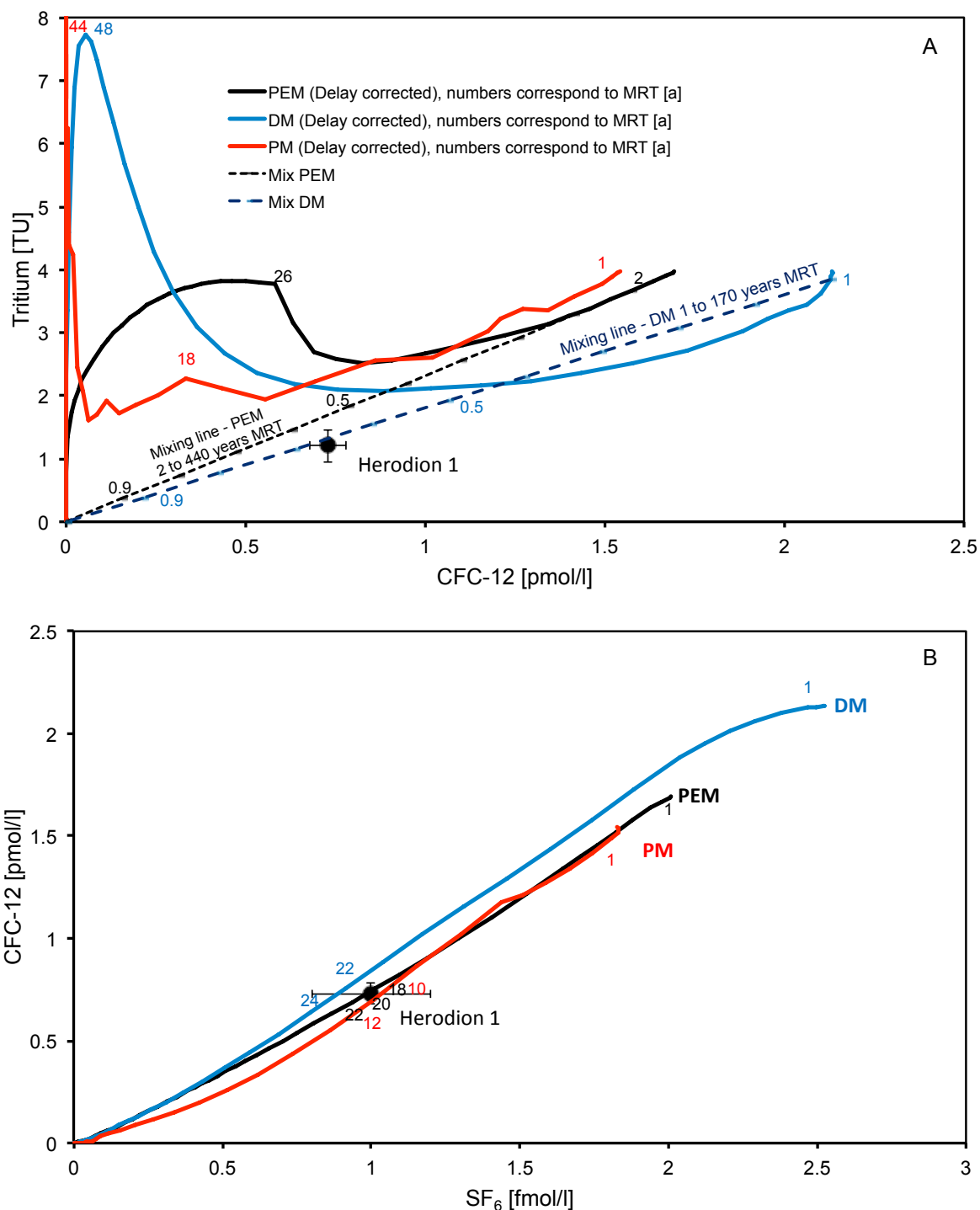


Figure 6: Modelling results for groundwater from Herodion 1 well, applying PM (red), PEM (black) and DM (blue) and (A) tritium vs. CFC-12 and (B) CFC-12 vs. SF₆. The calculated delays of CFC-12 are according 30 yrs., 20 yrs., and 28 yrs., to the models PM, DM and PEM, respectively (ref. Table 3).



4.3 Recharge rates and dual porosity

The mean residence times resulting from lumped parameter models PM, DM and PEM in Table 4 were used to calculate
470 recharge rates according to Equations (4) and (5). Within a single LPM the MRT have uncertainties in the range of 50% and
this uncertainty increases to approximately a factor of 2 if all models are regarded as equally probable (Table 4). Therefore, a
major uncertainty for the calculation of recharge results from the unknown porosity of the karst aquifer, which is estimated
to be somewhere between 2% and 20%, creating an additional uncertainty of a factor of ten. It is therefore useful to consider
whether this uncertainty can be further restricted.

475 Recharges rates from chloride mass balance (CMB) highly depend on the value used for chloride in precipitation since the
chloride concentration in the Cenomanian aquifer for youngest groundwater (tritium >1.5TU) varies only by 22% between
28 mg/l and 44 mg/l (Table 1). The Cl values measured in precipitation during the present study vary between 5 and 30 mg/l
resulting in a spread between 62 mm/a and 375 mm/a for the recharge derived from CMB according to Equation 7, assuming
an average precipitation amount of 550mm/y. This is comparable to recharge rates used in numerical flow modelling studies
480 of the eastern groundwater catchment at the Dead Sea, who estimated 124-292 mm/a (Guttman, 2000) and 100-300 mm/a
(Gräbe et al., 2013) in the mountainous recharge area.

Tracer-derived recharge values compare best with the recharge estimates from CMB and numerical modelling if a porosity
of 10% is assumed. The tracer-derived values for 20% porosity are in the range of 40% to 100% of the mean annual
precipitation of Jerusalem and especially the latter value seems unrealistically high. The highest values originate from the
485 PM and the PEM. The PM neglects mixing and retardation along the flow path completely, which of course is the least
probable assumption. The PEM, however, takes mixing in the well into account, but it relies on the flow system being
extremely homogeneous, as in the “Vogel” aquifer (Jurgens et al., 2016; Vogel, 1967). A few preferential flow paths can
easily disturb this picture towards smaller MRT and thus larger recharge values. An indication why the tracer-derived
recharge values using 2% porosity are unrealistically low comes from the hydrogeology of the karst aquifer itself. The 2%
490 porosity can be attributed to structural fractures and macropores in the limestone, which account for rapid reaction of the
groundwater surface to precipitation events (Jabreen et al., 2018). However, according to Equation (5) the tracers are not
expected to indicate this flow but they would be retarded by diffusion of tracer into and out of the rock matrix (Maloszewski
et al., 2004; Purtschert et al., 2013; Suckow et al., 2019). This means the tracers never “see” only the 2% fracture and
macropore space of the karst but also at least a part of the total rock matrix with its total porosity of rather 20%. If the
495 effective porosity in the karst system is 2% and the total porosity is 20%, the retardation factor according to equation 5
would be 10. Applied to the lumped parameter models, this retardation means that the calculated MRT are too old and the
calculated recharge rates with 2% porosity are too low.



500 **Table 5.** Results of recharge rates [mm/a] based on maximum and minimum of the estimated MRT [a] obtained from PM, DM and PEM for Samia 2.

Model	MRT	2% porosity	10% porosity	20% porosity
		Recharge [mm/a]	Recharge [mm/a]	Recharge [mm/a]
PM	MRT 9 a	51	256	511
	MRT 29 a	16	157	315
DM	MRT 16.3 a	28	141	282
	MRT 22.6 a	20	120	203
PEM	MRT 31 a	45	226	452
	MRT 45 a	31	156	311

5 Conclusions

The present study derived groundwater flow patterns, mixing end-members, transport times and recharge estimates in the upper and lower Cretaceous aquifers in Israel between the recharge area around the central mountain ridge and the discharge zones close to the lower Jordan Valley and the Dead Sea. This was possible, despite a very low number of measurements and a complicated karst hydrogeological setting, using a powerful combination of multiple lines of evidence from hydrogeology, hydrochemistry, anthropogenic organic trace substances and classical environmental age-dating tracers like tritium, CFCs, SF₆ and ³⁶Cl/Cl. The present study is one of presently only a handful demonstrating the useful application of atmospheric bomb-test derived ³⁶Cl to study groundwater movement. The lower Cretaceous aquifer was found to be basically free of tritium and other anthropogenic environmental tracers like CFCs, SF₆ and bomb-derived ³⁶Cl and, therefore, has groundwater transport times larger than 50 years. Groundwater in the upper Cretaceous aquifer contains anthropogenic trace substances, indicating time scales of groundwater flow of a few decades and shows clear indications of preferential flow paths as expected for karstified groundwater systems. In two springs the combination of several environmental tracers (³H, bomb-derived ³⁶Cl, CFC-11, CFC-12, CFC-113, SF₆) allowed estimates of the mean residence time in the saturated zone, gas transfer delays in the unsaturated zone and mixing ratios with older groundwater. These estimates were confirmed by anthropogenic substances from agriculture (nitrate and pesticides like Simazine®), pain killers (Naproxen®) and sweeteners (Acesulfame K®). Calculated recharge rates based on MRT estimates compare well with chloride mass balance and numerical flow modelling. The multi-tracer methodology presented here is applicable in other data sparse areas with complex hydrogeology (karst or fractured) with or without anthropogenic influence.

520



Acknowledgments

The authors are grateful for the support of the project, which was partly covered by the SUMAR project, funded by the German Ministry of Education and Research (grant code: 02WM0848) and by the DESERVE Virtual Institute (grant code VH-VI527) funded by the Helmholtz Association of German Research Centres. We wish to thank Prof. Yossi Yechieli for hosting and Dr. Avner Avalon from Geological Survey of Israel for sampling recent precipitation. We also want to thank Dr. Yossi Guttman, (Mekorot) and Mohammed Hadidoun (Palestinian Water Authority) for enabling sampling at the wells. We thank the Israel Hydrological Survey for providing support and well data. Parts of this research was carried out at the Ion Beam Centre at the Helmholtz-Zentrum Dresden-Rossendorf e.V., a member of the Helmholtz Association. We like to thank S.M.E. Baez, R. Ziegenrücker and the DREAMS operator team for supporting the AMS-measurements.

References

- Akhmadaliev, S., Heller, R., Hanf, D., Rugel, G., and Merchel, S.: The new 6MV AMS-facility DREAMS at Dresden, Nuclear Instruments and Methods in Physics Research Section B: Beam Interactions with Materials and Atoms, 294, 5-10, 2013.
- Allison, G. and Hughes, M.: The use of environmental chloride and tritium to estimate total recharge to an unconfined aquifer, Soil Research, 16, 181-195, 1978.
- Alvarado, J. C., Purtschert, R., Hinsby, K., Troldborg, L., Hofer, M., Kipfer, R., Aeschbach-Hertig, W., and Arno-Synal, H.: ^{36}Cl in modern groundwater dated by a multi-tracer approach (^3H , ^3He , SF 6, CFC-12 and ^{85}Kr): A case study in quaternary sand aquifers in the Odense Pilot River Basin, Denmark, Applied Geochemistry, 20, 599-609, 2005.
- Arany, E., Szabó, R. K., Apáti, L., Alapi, T., Ilisz, I., Mazellier, P., Dombi, A., and Gajda-Schrantz, K.: Degradation of naproxen by UV, VUV photolysis and their combination, Journal of Hazardous Materials, 262, 151-157, 2013.
- Avrahamov, N., Yechieli, Y., Purtschert, R., Levy, Y., Sültenfuß, J., Vergnaud, V., and Burg, A.: Characterization of a carbonate karstic aquifer flow system using multiple radioactive noble gases (^3H - ^3He , ^{85}Kr , ^{39}Ar) and ^{14}C as environmental tracers, Geochimica et Cosmochimica Acta, 242, 213-232, 2018.
- Bakalowicz, M.: Karst groundwater: a challenge for new resources, Hydrogeology Journal, 13, 148-160, 2005.
- Bayer, R., Schlosser, P., Bönisch, G., Rupp, H., Zaucker, F., and Zimmek, G.: Performance and blank components of a mass spectrometric system for routine measurement of helium isotopes and tritium by the ^3He ingrowth method, Sitzungsberichte der Heidelberger Akademie der Wissenschaften, Mathematisch-naturwissenschaftliche Klasse, 5, 241-279, 1989.
- Begin: Geological map of Israel, Jericho, Sheet 9-III, 1: 50,000, with Explanatory Notes, Geological Survey of Israel, Jerusalem, 1974. 1974.
- Bentley, H. W., Phillips, F. M., Davis, S. N., Habermehl, M. A., Airey, P. L., Calf, G. E., Elmore, D., Gove, H. E., and Torgersen, T.: Chlorine 36 Dating of Very Old Groundwater 1. The Great Artesian Basin, Australia, Water Resources Research, 22(13), 1991-2001, 1986.



- Berman, T., Isabella, K., and Shay, R.: Environmental Health in Israel 2014, Jerusalem: Ministry of Health, 2014. 2014.
- Beyerle, U., Aeschbach-Hertig, W., Imboden, D. M., Baur, H., Graf, T., and Kipfer, R.: A Mass Spectrometric System for
555 the Analysis of Noble Gases and Tritium from Water Samples, *Environmental Science & Technology*, 34, 2042-2050, 2000.
- Bullister, J. and Weiss, R.: Determination of CCl₃F and CCl₂F₂ in seawater and air, *Deep Sea Research Part A. Oceanographic Research Papers*, 35, 839-853, 1988.
- Cook, P. and Solomon, D. K.: Recent advances in dating young groundwater: chlorofluorocarbons, ³H₃He and ⁸⁵Kr, *Journal of Hydrology*, 191, 245-265, 1997.
- 560 Cook, P. and Solomon, D. K.: Transport of atmospheric trace gases to the water table: Implications for groundwater dating with chlorofluorocarbons and krypton ⁸⁵, *Water Resources Research*, 31, 263-270, 1995.
- Cook, P. G., Solomon, D. K., Plummer, L. N., Busenberg, E., and Schiff, S. L.: Chlorofluorocarbons as Tracers of Groundwater Transport Processes in a Shallow, Silty Sand Aquifer, *Water Resour. Res.*, 31, 425-434, 1995.
- Crosbie, R. S., Peeters, L. J. M., Herron, N., McVicar, T. R., and Herr, A.: Estimating groundwater recharge and its
565 associated uncertainty: Use of regression kriging and the chloride mass balance method, *Journal of Hydrology*, 561, 1063-1080, 2018.
- Davis, S. N., Bentley, H. W., Phillips, F. M., and Elmore, D.: Use of cosmic-ray produced radionuclides in hydrogeology, *EOS*, 64, 283, 1983.
- Eriksson, E. and Khunakasem, V.: Chloride concentration in groundwater, recharge rate and rate of deposition of chloride in
570 the Israel Coastal Plain, *Journal of Hydrology*, 7, 178-197, 1969.
- Ford, D. and Williams, P.: Introduction to Karst, *Karst Hydrogeology and Geomorphology*, 2007. 1-8, 2007.
- Garfunkel, Z., Zak, I., and Freund, R.: Active faulting in the dead sea rift, *Tectonophysics*, 80, 1-26, 1981.
- Ghanem, M.: Hydrogeology and hydrochemistry of the Faria drainage basin/West Bank, 1999. *Inst. für Geologie*, 1999.
- Gräbe, A., Rödiger, T., Rink, K., Fischer, T., Sun, F., Wang, W., Siebert, C., and Kolditz, O.: Numerical analysis of the
575 groundwater regime in the western Dead Sea escarpment, Israel+ West Bank, *Environ Earth Sci*, 69, 571-585, 2013.
- Guttman, J.: Multi-lateral project B: hydrogeology of the eastern aquifer in the judea hills and jordan valley, Mekorot Water Company, Report, 468, 36, 2000.
- Guttman, Y., Flexer, A., Hötzl, H., Bensabat, J., Ali, W., and Yellin-Dror, A.: A 3-D hydrogeological model in the arid zone of Marsaba-Feshchah region, Israel, 2004, 1510-1513.
- 580 Heikkilä, U., Beer, J., Feichter, J., Alfimov, V., Synal, H.-A., Schotterer, U., Eichler, A., Schwikowski, M., and Thompson, L.: ³⁶Cl bomb peak: comparison of modeled and measured data, *Atmospheric Chemistry and Physics*, 9, 4145-4156, 2009.
- Herut, B., Starinsky, A., Katz, A., Paul, M., Boaretto, E., and Berkovits, D.: ³⁶Cl in chloride-rich rainwater, Israel, *Earth and Planetary Science Letters*, 109, 179-183, 1992.
- Huysmans, M. and Dassargues, A.: Review of the use of Péclet numbers to determine the relative importance of advection
585 and diffusion in low permeability environments, *Hydrogeology Journal*, 13, 895-904, 2005.
- IAEA: Use of Chlorofluorocarbons in Hydrology. A Guidebook, International Atomic Energy Agency, Vienna, 2006.



- IAEA/WMO 2019: Global Network of Isotopes in Precipitation. The GNIP Database. Accessible at: <http://www.iaea.org/water>, 2019. 2019
- Jabreen, H., Wohnlich S., Banning A., Wisotzky F., Niedermayer A., Ghanem M.: Recharge, geochemical processes and water quality in karst aquifers: Central West Bank, Palestine. *Env. Earth Sci.* 2018 (6)
- Jurgens, B. C., Böhlke, J. K., Kauffman, L. J., Belitz, K., and Esser, B. K.: A partial exponential lumped parameter model to evaluate groundwater age distributions and nitrate trends in long-screened wells, *Journal of Hydrology*, 543, Part A, 109-126, 2016.
- Katz, A. and Kolodny, N.: Hypersaline brine diagenesis and evolution in the Dead Sea-Lake Lisan system (Israel), *Geochimica et Cosmochimica Acta*, 53, 59-67, 1989.
- Khayat, S., Hoetzi, H., Geyer, S., and Ali, W.: Hydrochemical investigation of water from the Pleistocene wells and springs, Jericho area, Palestine, *Hydrogeology Journal*, 14, 192-202, 2006a.
- Khayat, S., Hoetzi, H., Geyer, S., Ali, W., Knoller, K., and Strauch, G.: Sulphur and oxygen isotopic characters of dissolved sulphate in groundwater from the Pleistocene aquifer in the southern Jordan Valley (Jericho area, Palestine), *Isot. Environ. Health Stud.*, 42, 289-302, 2006b.
- Klein-BenDavid, O., Sass, E., and Katz, A.: The evolution of marine evaporitic brines in inland basins: The Jordan-Dead Sea Rift valley, *Geochimica et Cosmochimica Acta*, 68, 1763-1775, 2004.
- Lavastre, V., Salle, C. L. G. L., Michelot, J.-L., Giannesini, S., Benedetti, L., Lancelot, J., Lavielle, B., Massault, M., Thomas, B., Gilibert, E., Bourlès, D., Clauer, N., and Agrinier, P.: Establishing constraints on groundwater ages with ^{36}Cl , ^{14}C , ^3H , and noble gases: A case study in the eastern Paris basin, France, *Applied Geochemistry*, 25, 123-142, 2010.
- Lin, R. and Wei, K.: Tritium profiles of pore water in the Chinese loess unsaturated zone: Implications for estimation of groundwater recharge, *Journal of Hydrology*, 328, 192-199, 2006.
- Love, A., Herczeg, A. L., Sampson, L., Cresswell, R. G., and Fifield, L. K.: Sources of chloride and implications for ^{36}Cl dating of old groundwater, southwestern Great Artesian Basin, Australia, *Water Resources Research*, 36, 1561-1574, 2000.
- Lucas, L. L. and Unterwieser, M. P.: Comprehensive review and critical evaluation of the half-life of Tritium, *Journal of research-National institute of standards and technology*, 105, 541-550, 2000.
- Mahara, Y., Ohta, T., Kubota, T., Miyakawa, K., Hasegawa, T., Habermehl, M., and Fifield, L.: New dating method: Groundwater residence time estimated from the ^4He accumulation rate calibrated by using cosmogenic and subsurface-produced ^{36}Cl , 2012, 03002.
- Maloszewski, P., Stichler, W., and Zuber, A.: Interpretation of environmental tracers in groundwater systems with stagnant water zones, *Isotopes in Environmental and Health Studies*, 40, 21-33, 2004.
- Maloszewski, P. and Zuber, A.: Manual on lumped parameter models used for the interpretation of environmental tracer data in groundwaters, 2002.
- Maloszewski, P. and Zuber, A.: Determining the turnover time of groundwater systems with the aid of environmental tracers: 1. Models and their applicability, *Journal of Hydrology*, 57, 207-231, 1982.



- Merchel, S., Bremser, W., Alfimov, V., Arnold, M., Aumaître, G., Benedetti, L., Bourlès, D. L., Caffee, M., Fifield, L. K., Finkel, R. C., Freeman, S. P. H. T., Martschini, M., Matsushi, Y., Rood, D. H., Sasa, K., Steier, P., Takahashi, T., Tamari, M., Tims, S. G., Tosaki, Y., Wilcken, K. M., and Xu, S.: Ultra-trace analysis of ^{36}Cl by accelerator mass spectrometry: an interlaboratory study, *Anal Bioanal Chem*, 400, 3125-3132, 2011.
- 625 Möller, P., Rosenthal, E., Geyer, S., and Flexer, A.: Chemical evolution of saline waters in the Jordan-Dead Sea transform and in adjoining areas, *International Journal of Earth Sciences*, 96, 541-566, 2007.
- Mor, U. and Burg, A.: Geological map of Israel, Mizpe Shalem, Sheet 12-III ,1: 50,000 Geological Survey of Israel, Jerusalem, 2000. 2000.
- Müller, T., Osenbrück, K., Strauch, G., Pavetich, S., Al-Mashaikhi, K. S., Herb, C., Merchel, S., Rugel, G., Aeschbach, W.,
630 and Sanford, W.: Use of multiple age tracers to estimate groundwater residence times and long-term recharge rates in arid southern Oman, *Applied Geochemistry*, 74, 67-83, 2016.
- Oster, H., Sonntag, C., and Münnich, K. O.: Groundwater age dating with chlorofluorocarbons, *Water Resources Research*, 32, 2989-3001, 1996.
- Pavetich, S., Akhmadaliev, S., Arnold, M., Aumaître, G., Bourlès, D., Buchriegler, J., Golser, R., Keddadouche, K.,
635 Martschini, M., Merchel, S., Rugel, G., and Steier, P.: Interlaboratory study of the ion source memory effect in ^{36}Cl accelerator mass spectrometry, *Nuclear Instruments and Methods in Physics Research Section B: Beam Interactions with Materials and Atoms*, 329, 22-29, 2014.
- Plummer, L., Busenberg, E., and Cook, P.: Principles of chlorofluorocarbon dating. In: *Use of chlorofluorocarbons in hydrology: A guidebook*, 2006.
- 640 Purtschert, R., Yokochi, R., and Sturchio, N.: Krypton-81 dating of old groundwater. Chapter 5. In: *Isotope methods for dating old groundwater*, IAEA, 2013.
- Raz, E.: Geological map of Israel, 'En-Gedi, Sheet 16-I ,1: 50,000 Geological Survey of Israel, Jerusalem, 1986. 1986.
- Rebeix, R., Le Gal La Salle, C., Mayer, A., Finkel, R., Claude, C., Sültenfuß, J., and Simler, R.: ^{36}Cl deposition rate reconstruction from bomb pulse until present: A study based on groundwater records, *Applied Geochemistry*, 50, 199-208,
645 2014.
- Rosenfeld, A. and Hirsch, F.: The Cretaceous of Israel, *Geological Framework of the Levant*, 2, 393-436, 2005.
- Roth, I.: Geological Map of Israel, Wadi el Qilt, Sheet 12-I, 1: 50,000, with Explanatory Notes, *Geol Surv Israel*, Jerusalem, 1973. 1973.
- Rugel, G., Pavetich, S., Akhmadaliev, S., Enamorado Baez, S. M., Scharf, A., Ziegenrucker, R., and Merchel, S.: The first
650 four years of the AMS-facility DREAMS: Status and developments for more accurate radionuclide data, *Nuclear Instruments and Methods in Physics Research Section B: Beam Interactions with Materials and Atoms*, 370, 94-100, 2016.
- Schlosser, P., Stute, M., Dörr, H., Sonntag, C., and Münnich, K. O.: Tritium/ ^3He dating of shallow groundwater, *Earth and Planetary Science Letters*, 89, 353-362, 1988.



- Schmidt, S., Geyer, T., Guttman, J., Marei, A., Ries, F., and Sauter, M.: Characterisation and modelling of conduit restricted karst aquifers – Example of the Auja spring, Jordan Valley, *Journal of Hydrology*, 511, 750-763, 2014.
- Shachnai, E.: Geological map of Israel, Ramallah, Sheet 8-IV ,1: 50,000 The Israel Geological Survey, Jerusalem, 2000. 2000.
- Siebert, C., Rödiger, T., Mallast, U., Gräbe, A., Guttman, J., Laronne, J. B., Storz-Peretz, Y., Greenman, A., Salameh, E., Al-Raggad, M., Vachtman, D., Zvi, A. B., Ionescu, D., Brenner, A., Merz, R., and Geyer, S.: Challenges to estimate surface- and groundwater flow in arid regions: The Dead Sea catchment, *Science of The Total Environment*, 485-486, 828-841, 2014.
- Sneh, A. and Avni, Y.: Geological map of Israel, Jerusalem, Sheet 11-II, 1:50,000, Geological Survey of Israel, Jerusalem, 2011. 2011.
- Sneh, A. and Roth, Y.: Geological map of Israel, Hevron, Sheet 11-IV ,1: 50,000 Geological Survey of Israel, Jerusalem, 2012. 2012.
- Solomon, D. K., Poreda, R., Schiff, S., and Cherry, J.: Tritium and helium: 3 as groundwater age tracers in the Borden aquifer, *Water Resources Research*, 28, 741-755, 1992.
- Solomon, D. K., Poreda, R. J., Cook, P. G., and Hunt, A.: Site Characterization Using 3H/3 He Ground-Water Ages, Cape Cod, MA, *Groundwater*, 33, 988-996, 1995.
- Starinsky and Katz: The Story of Saline Water in the Dead Sea Rift – The Role of Runoff and Relative Humidity. In: *Dead Sea Transform Fault System: Reviews*, Garfunkel, Z., Ben-Avraham, Z., and Kagan, E. (Eds.), *Modern Approaches in Solid Earth Sciences*, Springer Netherlands, 2014.
- Stein, M., Starinsky, A., Katz, A., Goldstein, S. L., Machlus, M., and Schramm, A.: Strontium isotopic, chemical, and sedimentological evidence for the evolution of Lake Lisan and the Dead Sea, *Geochimica et Cosmochimica Acta*, 61, 3975-3992, 1997.
- Suckow, A.: The age of groundwater – Definitions, models and why we do not need this term, *Applied Geochemistry*, 50, 222-230, 2014a.
- Suckow, A.: Lumpy—an interactive lumped parameter modeling code based on MS access and MS excel, 2012, 2763.
- Suckow, A.: Lumpy - Lumped Parameter Modelling of Age Distributions using up to two Parallel Black Boxes. Software Manual., Leibniz Institute for Applied Geophysics (LIAG), S3, Geochronology and Isotope Hydrology, Hannover, 2014b.
- Suckow, A., Deslandes, A., Raiber, M., Taylor, A. R., Davies, P., Gerber, C., and Leaney, F.: Reconciling contradictory environmental tracer ages in multi-tracer studies to characterise the aquifer and quantify deep groundwater flow., *Hydrogeology Journal*, accepted for publication, 2019.
- Suckow, A., Sonntag, C., Gröning, M., and Thorweihe, U.: Groundwater recharge in the Umm Kedada Basin, NW-Sudan, derived from environmental isotopes of soil moisture in samples collected from deep dug wells. In: *Geoscientific Research in Northeast Africa*, Thorweihe, U. and Schandemeier, H. (Eds.), Balkema, Rotterdam, 1993.
- Sültenfuß, J. and Massmann, G.: Dating with the 3He-tritium-method: an example of bank filtration in the Oderbruch region, *Grundwasser*, 9, 221-234, 2004.



- Sültenfuss, J., Roether, W., and Rhein, M.: The Bremen mass spectrometric facility for the measurement of helium isotopes, neon and tritium in water, *Isotopes in Environmental and Health Science (Isotopenpraxis)*, 45, 83-95, 2009.
- 690 Synal, H. A., Beer, J., Bonani, G., Suter, M., and Wölfli, W.: Atmospheric transport of bomb-produced ^{36}Cl , *Nuclear Instruments and Methods in Physics Research Section B: Beam Interactions with Materials and Atoms*, 52, 483-488, 1990.
- Tosaki, Y., Massmann, G., Tase, N., Sasa, K., Takahashi, T., Matsushi, Y., Tamari, M., Nagashima, Y., Bessho, K., and Matsumura, H.: Distribution of $^{36}\text{Cl}/\text{Cl}$ in a river-recharged aquifer: Implications for the fallout rate of bomb-produced ^{36}Cl , *Nuclear Instruments and Methods in Physics Research Section B: Beam Interactions with Materials and Atoms*, 268, 695 1261-1264, 2010.
- Tosaki, Y., Tase, N., Massmann, G., Nagashima, Y., Seki, R., Takahashi, T., Sasa, K., Sueki, K., Matsuhira, T., Miura, T., Bessho, K., Matsumura, H., and He, M.: Application of ^{36}Cl as a dating tool for modern groundwater, *Nuclear Instruments and Methods in Physics Research Section B: Beam Interactions with Materials and Atoms*, 259, 479-485, 2007.
- Trettin, R., Knöller, K., Loosli, H., and Kowski, P.: Evaluation of the sulfate dynamics in groundwater by means of 700 environmental isotopes, *Isot. Environ. Health Stud.*, 38, 103-119, 2002.
- Vogel, J. C.: Investigation of groundwater flow with radiocarbon. , *Isotopes in Hydrology*, Vienna, 355-368, 1967.
- Wood, W. W. and Sanford, W. E.: Chemical and isotopic methods for quantifying ground-water recharge in a regional, semiarid environment, *Groundwater*, 33, 458-468, 1995.
- Yechieli, Y.: Fresh-Saline Ground Water Interface in the Western Dead Sea Area, *Ground Water*, 38, 615-623, 2000.
- 705 Yellin-Dror, A., Guttman, J., Flexer, A., Hötzl, H., Ali, W., and Bensabat, J.: 3.3. 2. 3-D Hydrogeological model of the Marsaba-Feshkha region, *The Water of the Jordan Valley: Scarcity and Deterioration of Groundwater and its Impact on the Regional Development*, 2008. 287, 2008.